Scientific Research Publishing

Open Journal of Geology, 2026, 16(7), 361-392
https://www.scirp.org/journal/ojg
ISSN Online: 2161-7589
ISSN Print: 2161-7570

# Rio Grande Relay Zone, Rio Grande do Sul Coastal Plain, Brazil: II—Asymmetric Delta Development and Gravity Fault Subsidence in Quinta-Cassino Strandplain

**Adelir José Strieder[1,2*], Iran Carlos Stalliviere Corrêa[3], Bruno Silva da Fontoura[4], Ana Carolina O. dos Santos[5], Paulo Rogério Mendes[6], Alexandre Felipe Bruch[4], Angélica Cirolini[7], José Antonio Scotti Fontoura[8]**

[1]Centro de Excelência em Geoinformática e Computação Visual (VIZLAB), Universidade do Vale do Rio dos Sinos (UNISINOS), São Leopoldo, Brazil
[2]STR Data & Geologia Ltda., Ijuí, Brazil
[3]Programa de Pós-Graduação em Geociências (PPGEO), Instituto de Geociências, Universidade Federal do Rio Grande do Sul (UFRGS), Porto Alegre, Brazil
[4]Engenharia Geológica, Centro de Engenharias, Universidade Federal de Pelotas (UFPel), Pelotas, Brazil
[5]Geofísica, Campus Caçapava do Sul, Universidade Federal do Pampa (UNIPAMPA), Caçapava do Sul, Brazil
[6]HIDROSERV-Serviços Geológicos e Geofísicos Ltda., Porto Alegre, Brazil
[7]Colégio Politécnico, Campus Camobi, Universidade Federal de Santa Maria (UFSM), Santa Maria, Brazil
[8]Escola de Engenharia, Universidade Federal de Rio Grande (FURG), Rio Grande, Brazil
Email: *adelirstrieder@outlook.com

**How to cite this paper:** Strieder, A.J., Corrêa, I.C.S., da Fontoura, B.S., dos Santos, A.C.O., Mendes, P.R., Bruch, A.F., Cirolini, A. and Fontoura, J.A.S. (2026) Rio Grande Relay Zone, Rio Grande do Sul Coastal Plain, Brazil: II—Asymmetric Delta Development and Gravity Fault Subsidence in Quinta-Cassino Strandplain. *Open Journal of Geology*, **16**, 361-392.
https://doi.org/10.4236/ojg.2026.167020

**Received:** May 12, 2026
**Accepted:** July 26, 2026
**Published:** July 29, 2026



## Abstract

This paper describes and characterizes the Rio Grande Relay Zone as a complex structural area developed due to the interaction of the north tips of the Quinta Main Listric and south tips of the Retiro-Estreito splaying and bending faults in the Rio Grande do Sul Coastal Plain (RGSCP). The paper characterizes the structural control for the Holocene lagoon-barrier system in the central to south RGSCP, based on recently identified gravity sliding faulting. The investigated area includes mainly the Quinta-Cassino area to the south of the Rio Grande channel and the Retiro area to the north of the channel. Gravimetric data, seismic lines, GPR lines and drillholes were used to evaluate and to re-interpret some previous results to highlight the structural features developed by that fault's interaction. Gravimetric data supported evidence that the Rio Grande Fault separates the deep Pelotas Basin, as well as the Rio Grande Structural High. The Quinta Main Listric and Retiro-Estreito Main faults are the consequence of crystalline basement tilt due to regional basin flexural subsidence. The basement tilt triggered gravity sliding tectonics from the Miocene to the Holocene. The Rio Grande High, on the other hand, set sedimentary loading anisotropies to control the listric normal faults propagation (splaying and bending). The interaction of subsided hangingwall of the Quinta Main Listric Fault and its subsidiary ones with the footwall block of the Retiro-Estreito Main Fault gave rise to a wedge-like locally subsided area and to an asymmetric delta, the Quinta-Cassino strandplain. The Rio Grande discharge channel was initially set close to Quinta Main Listric Fault scarp and was meandering according to the ramp relays in the Retiro-Estreito Fault footwall block to its actual discharge position. The Quinta-Cassino beach ridge progradation was cut by subsidiary listric faults, so that each fault block shows its own vertical sedimentation rates and a given time of displacement.

## Keywords

Gravity Sliding Tectonics, Local Subsidence and Structural Barriers, Normal Fault and Sedimentation, Holocene Asymmetric Delta Development

## 1. Introduction

The gravity tectonic is not a recent subject in the Pelotas Basin, but a well-known tectono-structural activity since the Miocene. [1] [2] recognized that "*relevant structures correspond to active system faults until the Late Pleistocene*". [3] has also recognized faults crosscutting Holocene units in seismic sections. [2] emphasized that "*Rio Grande Cone constitutes a huge sedimentary package characterized by the result of channel system morphology*, *sediment waves and contourites that have been influenced on the upper sequences by a distensional fault system that originated normal faults to the North and inverse faults to the South*". Even though deformation records were made in the offshore Pelotas Basin, those studies focused on seismic-stratigraphic units, depositional patterns, and the broader processes controlling subsidence and sediment input. The propagation of gravity tectonic structural features to the Rio Grande do Sul Coastal Plain (RGSCP) has also been reported [4] [5], but their investigations lack more detailed surveys.

[5]-[9] presented the role that recently identified gravity sliding normal faults had on controlling the Holocene sedimentary processes on the RGSCP (**Figure 1**). [10] had also shown important gravity sliding structures in the onshore platform and continental slope at the Rio Grande Cone (Pelotas Basin, RS, Brazil), developed from Miocene to present.

The main normal faults recently identified in the RGSCP are (**Figure 1**): 1) Quinta Main Listric Fault [6], 2) Lagoa do Peixe Listric Growth Fault [7], and 3) Retiro-Estreito Main Fault [8] [9]. All of them extend for >60 km, show an arcuate trace in plain view and present a listric profile with different deepening curvature. They also show different hangingwall block mechanical subsidence structural architecture: while Lagoa do Peixe Listric Growth Fault presents poor hangingwall faulting and space problem was accommodated by hangingwall rotation, the space problem in Quinta and Retiro-Estreito main listric normal faults was accommodated by fault splaying and bending[1].

The interaction of the southern tip zone of Lagoa do Peixe Listric Growth Fault [7] and the northern tip zone of Retiro-Estreito normal Fault [8] developed a structural high (the anticline due to hangingwall rotation) that primarily acted as structural barrier for Holocene deposits, and both normal faults interact and overlap at the Bujuru District area close to the Atlantic Ocean beach. However, poor normal fault splaying and bending were recorded in this tip and overlapping area. The Holocene transgressive dune field barrier (TD), then, was built upon the primary structural barrier and hosts Bujuru HM deposit [8].

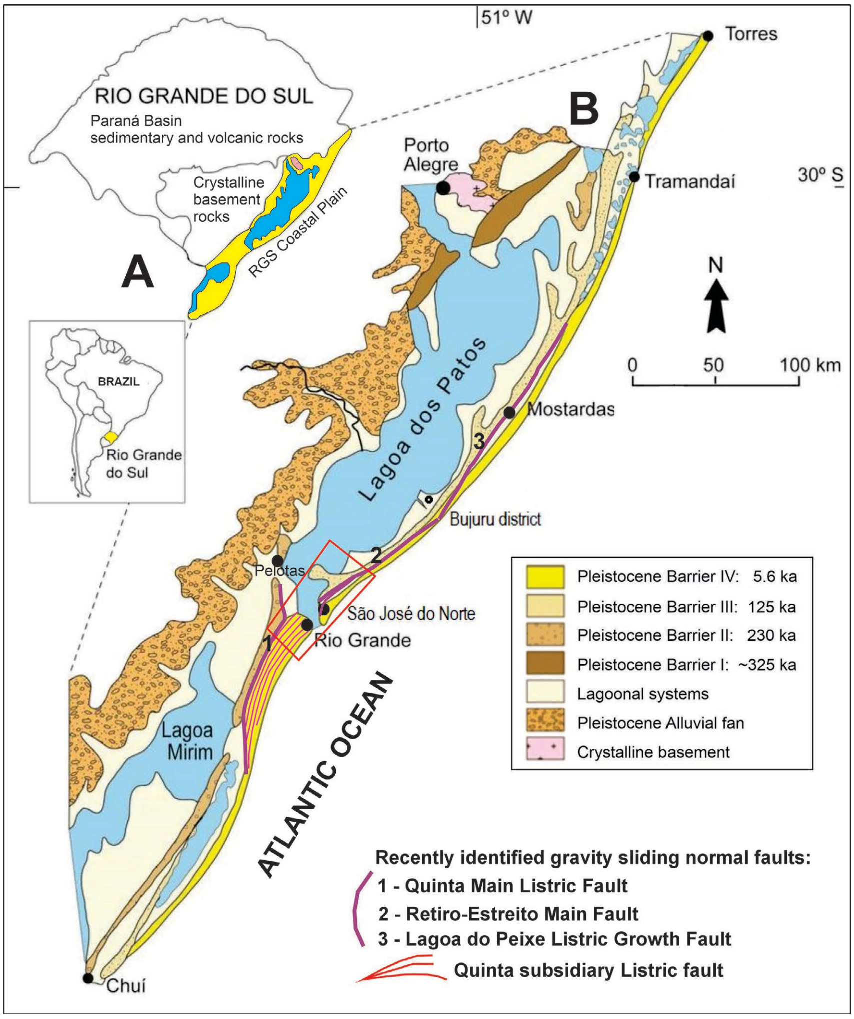


**Figure 1.** Rio Grande do Sul Coastal Plain location (A), and its regional geological map (B), as modified from [11] [12]. Lagoon/Barrier system ages according to [13]. The red rounded rectangle circumscribes the area of investigation in **Figure 2**. For details on gravity sliding structures, refer to [6] [9].

The southern tip zone of Retiro-Estreito Main Fault, on the other hand, shows

[1]Bend in normal fault refers to a change in fault strike, as seen in map view. Splay: Refers to a given number of subsidiary fault(s) that join a master (main) fault. In gravity tectonics, they usually join deepest segment of listric faults.

higher fault density, a much higher fault bending and splaying [9], but does not show an anticline structural barrier near the ocean beach, as recorded in the Lagoa do Peixe and Bujuru areas. The identified structural high in the southern Retiro-Estreito Main Fault tip zone is the fault scarp only, recorded as a narrow Retiro Horst to the west of São José do Norte town [9], which is part of the footwall block for Retiro-Estreito Main Fault.

The same faulted structural framework is observed to the south of Rio Grande channel: 1) the structural high is far west in the Quinta Listric Fault scarp [6], which is its footwall block, and 2) no structural anticline barrier close to ocean beach, due to space accommodation was solved by normal fault bending and splaying.

The interaction zone between the southern tip zone of Retiro-Estreito Main Fault [8] [9] and the northern tip zone of Quinta Listric Fault [6] is at the Rio Grande channel, actually an inlet channel connecting Lagoa dos Patos to Atlantic Ocean (**Figure 2**). To the south of this channel, controlled by the Quinta Listric Fault, a wide (~18 km) Holocene strandplain was developed [6]. The Quinta-Cassino strandplain narrows to the south (~1 km) and is composed of at least 18 sets of coastal ridges [14], which can be grouped into 7 stages [15] [16].

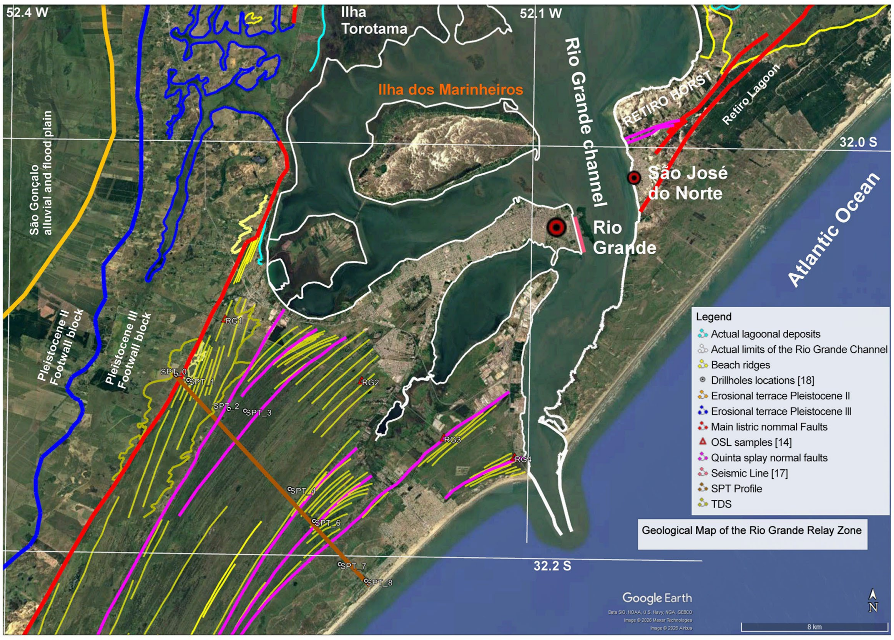


**Figure 2.** Geology of the Rio Grande Relay Zone, on both sides of Rio Grande channel. This map details geological features earlier presented by [6] [9], and locates some previous investigations results shown by [14] [17] [18], which will be discussed later in this paper.

The Rio Grande area, then, is the locus for Retiro-Estreito Main Fault and the Quinta Main Listric Fault interaction and overlapping, *i.e.*, a structural relay zone. It is noteworthy that the Quinta-Cassino strandplain ends abruptly against the Lagoa dos Patos (lagoon) and Rio Grande channel (**Figure 2**). The structural difference between the southern (Quinta Fault and its strandplain) and the northern

(Holocene lagoon-barrier fault-controlled system in Retiro area) requires additional investigations and discussions.

The aim of this paper is to evaluate some published data on Holocene RGSCP, as well as to analyse and discuss geological (sedimentary and structural) elements that enable understanding the structural differentiation and the development of the asymmetric delta in the Quinta-Cassino strandplain (RGSCP, Brazil). GPR surveys, drillholes, geochronological and field surveys data from published papers (e.g., [1]-[9] [14]-[20]) were evaluated to investigate this regional structural differentiation. Available gravity data and maps [10] were also used to further evaluate the basement features that can control RGSCP fault propagation.

The aim of this paper is also to complement and expand initial discussions introduced in [6], especially regarding the termination of normal splay faults in Quinta-Cassino strandplain and their structural sequence. Then, the paper discusses the fault propagation in the Quinta-Cassino strandplain and its control on sedimentation processes.

## 2. The Basement Structure for the RGSCP: A Review and Discussion

The RGSCP extends along ~600 km from southern Brazilian border to the northeast in the Santa Catarina state (Brazil). It widens progressively from ~20 km in the south, to ~100 km in the Porto Alegre region, and sharply narrows to 10 - 15 km in the Santa Catarina state.

The RGSCP is the emersed segment of the Pelotas Basin, the southernmost Atlantic-type passive margin in Brazil. Pelotas Basin can be divided into two segments: 1) a shallow basin, including the RGSCP and near offshore shelf, and 2) a deep basin, from the middle of the continental shelf to continental slope and continental rise [19]. These segments are separated by the Rio Grande Fault, a normal fault on basement rocks (Sul-Riograndense Shield and continental Paraná Basin) for Pelotas Basin, developed during the Atlantic Ocean opening [19]. The Rio Grande Fault runs parallel to the coast and was first identified by [19] through reflection seismic, gravity, and aeromagnetic surveys carried out by PETROBRAS in the Pelotas basin. The position of the Rio Grande Fault was later refined by previous data revaluation and refraction seismic surveys results [20].

The structural framework for the crystalline basement of Pelotas Basin can also be evaluated by means of gravity maps, especially the shallow basin. The gravity maps for the SE and NE onshore basement and Pelotas Basin itself (**Figure 3**) show the structural features in the shallow basin. These maps are from [10] and result from merging different gravity databases, after transformation of Coordinates and altimetry to a single geodetic system (SIRGAS 2000.4), and joint determination of Bouguer anomaly from original gravity measurements.

The Rio Grande Fault can be easily recognized in the Bouguer gravity (**Figure 3(A)**) and in its first derivative (**Figure 3(B)**) maps. It is best defined close to Mostardas, where onshore and offshore gravity surveys are close together. The Rio

Grande Fault is set just in the high negative gravity gradients in the first derivative map (Figure 3(B)). As previously defined [19] [20], it separates the shallow and deep Pelotas Basin.

Figure 3(C) offers an interpretative approach for the geometry of these basement structures over which shallow Pelotas Basin was developed. Based on Bouguer anomaly and its first derivative maps, two main re-entrant features can be identified in the onshore shallow Pelotas Basin (Figure 3(B), Figure 3(C)), which correspond to RGSCP. These re-entrant features can be defined by arcuated linear traces displaying a high gravity gradient from positive to negative values (Figure 3(B)). The high Bouguer gravity values circulating the re-entrances are well identified by outcropping crystalline basement in the São Lourenço do Sul and Tapes cities for example.

Both these re-entrances can be interpreted as two half-graben features [21] [22] in the Pelotas Basin: 1) the southern Taim half-graben, and 2) the central-north Bujuru half-graben. They are separated by a gravimetric high well defined in the Bouguer anomaly map (Figure 3(A)), whose extension is seen in its first derivative map (Figure 3(B)). This gravimetry high is related to a drillhole in the Rio Grande (522 m to basement) area, which is long known as a structural high: the Rio Grande structural and gravimetric high [19].

The southern Taim half-graben is characterized by low gravimetric gradients (0.0002 - 0.0007 mGal/m) along the entire segment, which are in accordance with gneissic-granitic basement depth from drillholes. To the west, it is limited by two elongated strips that may suggest steps in the half-graben [22] [23]. In this area, the RGSCP sediments were deposited upon a near-surface crystalline basement. Four drillholes for oil and gas determined the depth to basement (156 and 320 in the Lagoa Mirim area, 210 in Pelotas, and 522 in Cassino area). The Taim half-graben was the locus for Quinta-Cassino strandplain development.

The central-north Bujuru half-graben, however, is not as elongated and has significant variation in the gravimetric gradients (0.0000 - 0.0017 mGal/m). It is limited to NE by a gravimetric high extending from Camaquã, Tapes to Mostardas region. The east limit of this gravimetric high coincides with the northern tip of the Lagoa do Peixe Growth Fault. This shallow Pelotas basement features controls on the Retiro-Estreito Main Fault and also the Lagoa do Peixe Growth Fault [6] [8]. In the Bujuru half-graben area, low gravity values extend toward the west, and greater depths to basement are recorded. In the Mostardas area, the drillholes reached gneissic basement at 1517 m depth, and basaltic basement at 3500 m depth, which is explained by the Rio Grande fault bending abruptly toward Mostardas town [20].

The geometry of this re-entrant gravity linear gradient is consistent with half-grabens described in East African Rift [22] [23], prior to complete continental breakup. The gravity features suggest that Taim half-graben is filled with a thinner RGSCP sedimentary sequence, while the Bujuru half-graben has a thicker sedimentary sequence and highly variable gravimetric gradients.

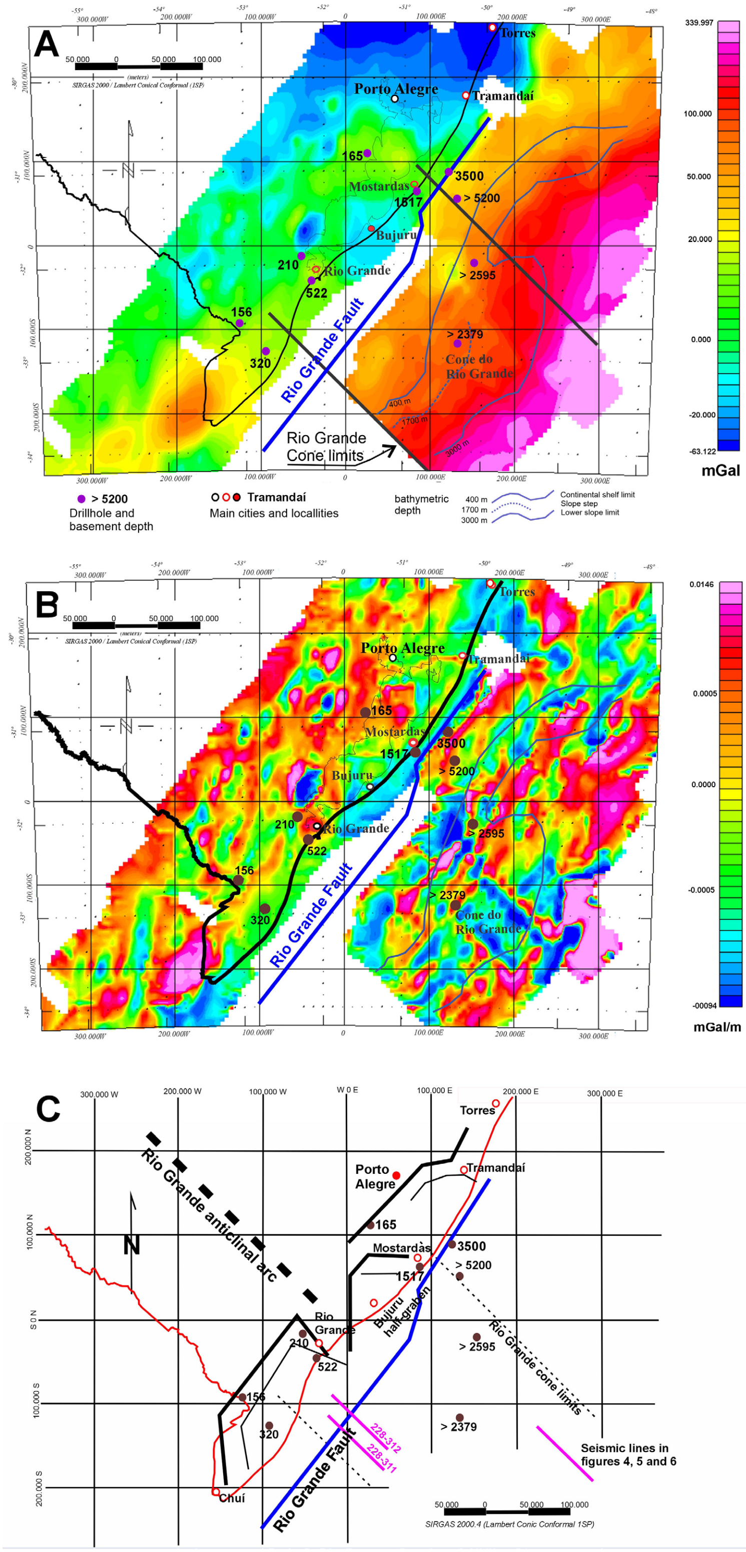


**Figure 3.** Gravity maps for the Pelotas Basin, including its basement (Paraná Basin and Sul-riograndense Shield) to the west [10]. (A) Bouguer map; (B) First derivative of Bouguer map; (C) Structural crystalline basement interpretation related to Atlantic Ocean opening. Gravity data were compiled from ANP and IBGE (Brazil), and BGI; they were corrected for SIRGAS (2000.4) altimetry and the Bouguer anomaly was then recomputed.

The first derivative gravity map (**Figure 3(B)**) emphasizes the near-surface gravity sources and shows that southern and central-north segments of the RGSCP (onshore shallow Pelotas Basin) have distinguishing basement properties. It is also to be noted that the Rio Grande structural and gravimetric high is aligned to Rio Grande Arc, a broad regional NW deeping anticlinal developed during the second deformational phase recognized in the Serra Geral Fm., the Paraná-Etendeka Flood Basalt Province [23].

The northern tip zone of the bending and splaying normal faults in the Quinta-Cassino strandplain [6] and the southern tip zone for Retiro-Estreito Main Fault [8] seems to be controlled by Rio Grande structural and gravimetric High. Then, the Rio Grande Relay Zone for these normal listric faults relates to the Rio Grande High.

## 3. Discussion on Tectonics and Subsidence in Pelotas Basin: A Review

An Atlantic-type passive margin basin, such as Pelotas Basin, can be characterized as evolving from 1) continental rift, to 2) nascent ocean basins and continental margins, and to 3) intraplate continental margins stages [24], or drift stage. The corresponding "*subsidence mechanisms evolve from* 1) *thinning of continental crust by stretching and erosion during doming and rifting*, *to* 2) *thermal subsidence following rifting as the intraplate margin moves away from the spreading ridge*, *to* 3) *both local crustal and regional lithospheric sediment loading during the later history of the intraplate continental margin*" [24]. In this way, thick-skinned extensional tectonic structures [22] from rifting and immediate post-rift stages (large-scale local mechanical subsidence) are not to be confused with thin-skinned tectonics [25] [26] developed in the flexural stage (mostly regional mechanical subsidence) due to sedimentary loading (drift stage).

The Rio Grande Fault [19] [20] and the Taim and Bujuru half-grabens are the initial results from Atlantic Ocean opening and are part of a thick-skinned process (Gondwana Plate divergence and rupture). The stress field for this process is not governed by Earth's gravity.

Gravity tectonics, a term applied interchangeably with gliding tectonics or gravity slide tectonics, refers to the processes by which large blocks or slabs of the Earth's crust move under the dominant influence of gravity [27]. Gravity tectonics, then, is classified as a thin-skinned group of structural features developed in response to flexural mechanical subsidence in the intraplate continental margin's stage [28]. Flow of a plastic or viscous layer can be driven by gravity, in response to sedimentary loading and tilting of the base of such layer during this evolution stage of the basin, and the triggering mechanisms are diverse [27] [29]-[31].

The thin-skinned, gravity tectonic structural features in Rio Grande Cone of Pelotas Basin were recently analysed in detail [10], and some results are shown in **Figures 4-6**. **Figure 4** shows a seismogram surveyed just in front of Quinta-Cassino strandplain, clearly depicting a large complete rotational spreading structure developed from Miocene to Holocene [10]. The upper segment of the continental slope and platform displays local extensional normal faults, while the lower segment accommodates compressional inverse thrust faults and folds. The main deformation is concentrated in the platform slope, but normal faults sequentially propagate toward the continental margin [10].

Figure 5 shows the seismic reflectors thickening in the downward-sinking space generated by the main normal faults [10]. This feature is developed when downward throw rate is greater than sedimentation rate. It is related to the growth fault development.

Figure 6, in addition, shows superposed sliding thrust blocks deforming Holocene sediments seaward from Quinta-Cassino strandplain [10]. This structure was also described as Chuí Megaslide Complex [32], distinguishing its connected extensional and compressional segments.

Figures 4-6, then, show some examples of thin-skinned gravity tectonic structures developed up to Pelotas Basin Holocene epoch. These structural features are consequence of regional subsidence (flexural mechanisms) supported in the deep Pelotas Basin [19] [20] during the intraplate continental margin's stage. These features differ from Rio Grande Fault in that this previously recognized fault [19] [20] was developed during the Atlantic Ocean rifting stage (it is the result of the thick-skinned tectonics).

Careful observation, therefore, must be exercised to avoid confusing thick-skinned tectonic features and local mechanical subsidence with thin-skinned tectonic features and regional flexural subsidence due to sedimentary load.

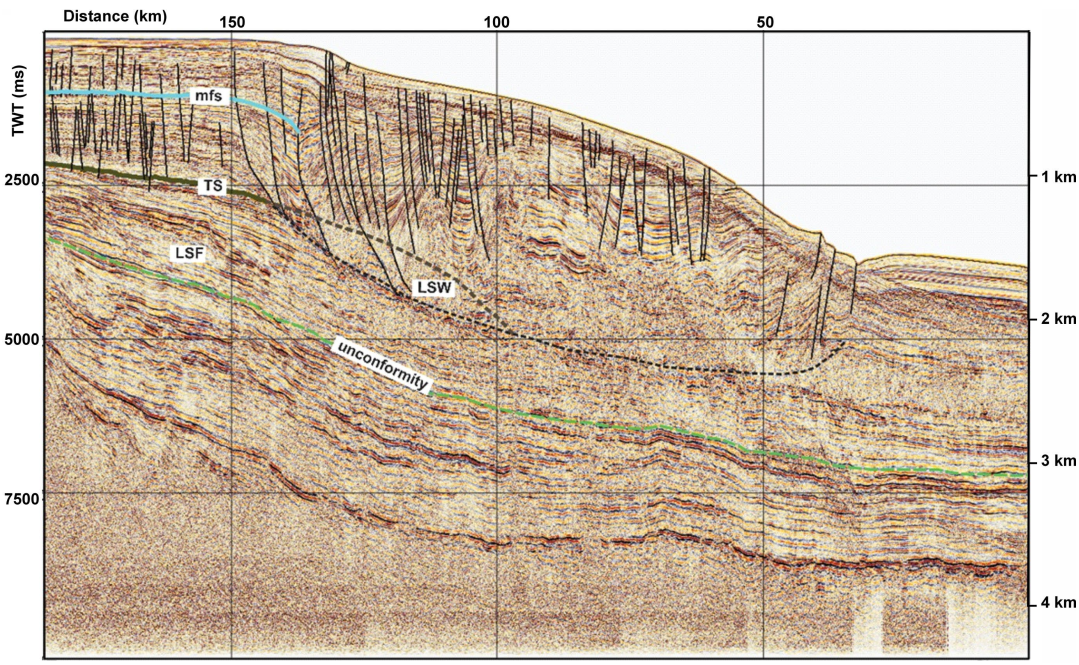


Figure 4. Seismogram "228_312" (orange line in location map in the upper right corner) showing the gravitational collapse and spreading of the south segment of the Rio Grande Cone (Pelotas Basin, Brazil) eastward of Quinta-Cassino strandplain [10]. Some preliminary references: The green line is the Miocene unconformity; the dark green **TS** is a Transgressive Surface; **LSF** is a Lowstand Fan; **LSW** is the Lowstand Wedge; and **mfs** is the maximum flooding surface. The dotted line is the basal detachment fault surface of the thin-skinned structure.

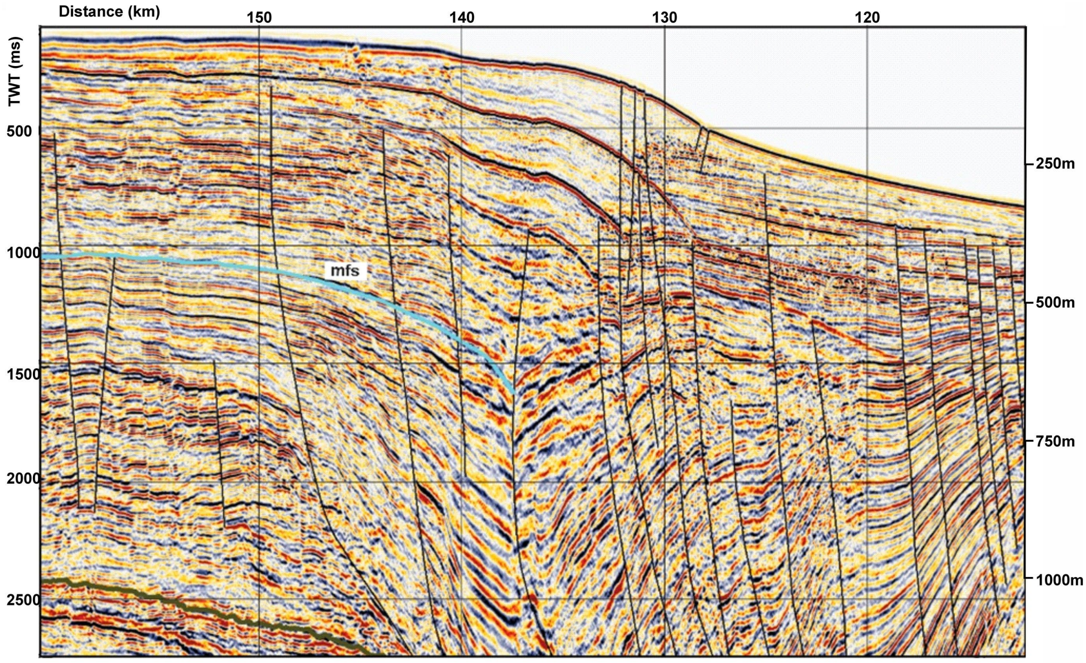


**Figure 5.** Detail of the upper extensional segment of the gravitational collapse and spreading structure shown in **Figure 4** (seismogram "228_312"), which put into evidence the thickening of reflectors near the normal faults. The black lines represent the main normal faults in the section. The blue line represents the preliminary reference for maximum flooding surface (**mfs**) [10].

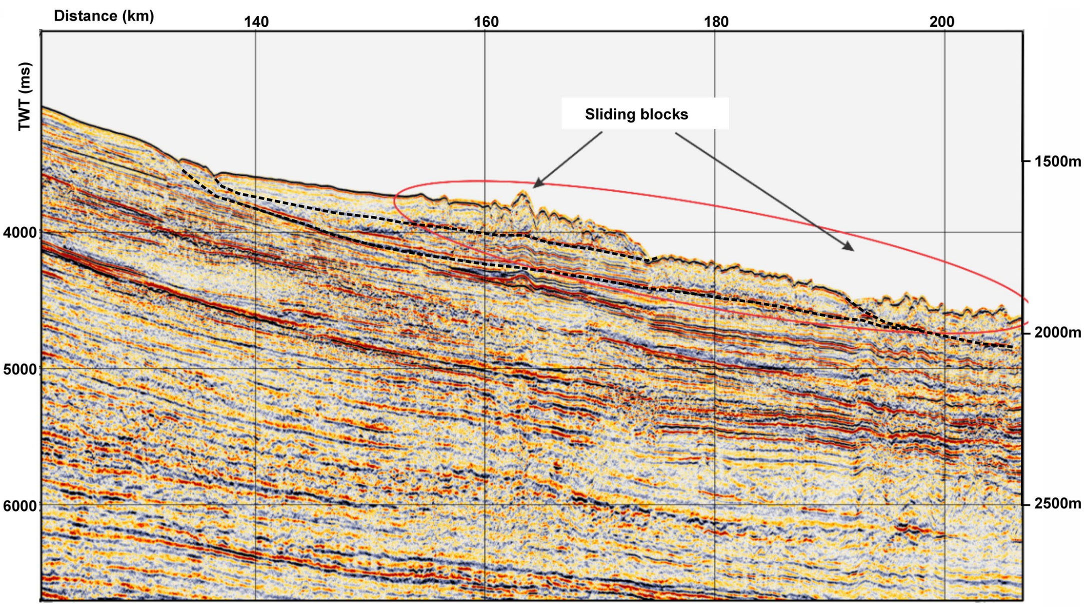


**Figure 6.** Seismogram "228_311" (orange line in location map in the upper right corner) showing the gravitational sliding of the south segment of the Rio Grande Cone (Pelotas Basin, Brazil) eastward of Quinta-Cassino strandplain [10]. The red ellipse emphasizes the compressional frontal segment folding Holocene sediments. The black dashed lines emphasize Holocene master faults.

Flexural subsidence of Brazilian passive margin basins nowadays set in plate interior has long been recognized [33]: "*In the southeast continental margin of*

*Brazil, a seismic zone extends from Rio Grande do Sul to Espírito Santo, with seismic activity occurring mainly along the continental slope and suggesting a close relationship with flexural stresses caused by the weight of the sediments*".

[3] [34] provided a robust subsidence analysis for Pelotas Basin, showing that the "*subsidence evolution during the syn-rift to drift basin stage of the southern Brazilian margin has been analyzed by numerical modeling* (*inverse basin modeling, 2D flexural backstripping*)". [3] [34] distinguished six subsidence trends (STs), and the Pelotas Basin turned to behave as an intracontinental basin from ST4 on. "*The sixth subsidence trend* (*ST*6) *lasts from the early Miocene* (23 *Ma*) *until today*"; this period is characterized by an initial subsidence decrease (10 - 40 m/m.y.), and a strong subsidence increase from the Tortonian to present (up to 110 m/m.y.) [34].

The Tertiary (drift stage) subsidence "*pattern correlates with high sediment input and therefore increased flexural loading*" [3]. "*Flexural sediment loading amplified slope gradients and intermittent turbidite deposition persisted throughout the … Tertiary*" [34]. "*The … middle-upper Miocene retrogradation* (…) *resulted from increasing subsidence and a second order eustatic sea-level rise exceeding the rates of sediment supply. An intra-late Miocene* (9 *Ma*, *Tortonian*) *maximum flooding surface* (*mfs*) *marks a shift to aggradation-progradation* (…). *This depositional trend persists until today*" [3].

Several mechanisms can trigger gravity tectonics [27] [29]-[31]. However, the regional flexural subsidence due to sedimentary loading in continental passive margin basin can additionally increase the continental shelf slope ($\beta$). [35] pointed out that continental passive margin displaying slopes as low as 0.01˚ can still trigger thin-skinned tectonics. That's to say, the basement tilt would be in control.

The [3] [34] results, then, show that regional-scale subsidence in the Pelotas Basin, from Tertiary until today, was controlled by flexural sedimentary loading. This regional-scale mechanical subsidence amplifies continental shelf and slope gradients to induce different kinds of mass-transport deposits (MTD): sliding, gliding, debris flows, turbidites, and others. It is noteworthy that extensional upper segment of sliding and gliding structures produces local mechanical subsidences, that would be filled by locally thickened sediments, specially under high sediment influx, as identified in the Tortonian to present period of the Pelotas Basin [3] [34].

## 4. Quinta-Cassino Strandplain Data and Evolution Discussion

Some previously published data lack for complete radargram processing, and then, were misinterpreted. These data have large importance for understanding the gravity tectonics process in the Quinta-Cassino strandplain. In this way, those previously published data are here evaluated, and a new interpretation is proposed.

[18] presented some radargrams (e.g., their Figure 6(B) and Figure 7) to support their radarfacies interpretation and suggested a "*complex relation between the*

*transgressive and regressive phases at the inner part of the Cassino barrier*". It is to be noticed that those radargrams present two basic problems:

1) There is not a two-way travel time y-axis (opposed to depth converted one), so that readers can easily evaluate the time-depth conversion and some processing procedures.

2) The radargrams show a very large number of diffraction hyperboles. According to [18], "*The data were post-processed with* […] *background removal and the application of bandpass frequency filters, an Ormsby bandpass filter, gain equalization, topographic corrections and time-to-depth conversion*". [18], then, did not apply any migration technique to collapse diffraction hyperboles, keeping many artifacts that make it hard to interpret reflectors continuity and truncations[2].

The diffraction hyperboles are too close in some areas of those radargrams [18] so that their tails interfere to eliminate some of the underground reflections. There exist curved reflectors also producing (reflection) hyperboles and destructive interferences in their inner parts and along tails. The problem of diffractions in faulted blocks is an old task in seismic data processing [36] [37], as it is in so many other geological structures imaged through wave propagation geophysical methods. There exist several migration techniques to solve these interference patterns, which apply both for seismic ([38], pp. 243-246) and for radar ([38], pp. 554-560) methods.

An evaluation of migration impact can be seen in companion paper (Figure 3 in [9]). In case of GPR unshielded and not well-grounded antennas, aerial waves will produce strong diffraction hyperboles in any surface objects, besides diffraction in underground irregularities and structures.

It is, then, "*Of particular significance is the ability to restore correct subsurface geometric relationships through the process of migration. Diffraction hyperbolae can be migrated back to the apex from which the diffraction originated. Dipping planar surfaces can be corrected to their correct position relative to ground locations. Otherwise, significant errors can be made by believing that the location of a particular subsurface feature on a raw radargram is exact, whereas it is only a virtual image and may be displaced from its actual position by significant horizontal and vertical distances*" ([38], p. 558).

The non-migrated radargrams pose limitations for direct radarfacies interpretation based only on radargram images. The raw data from [18] is not available for a new post-processing. In this way, some conclusions in radargrams interpretation are preliminary, even though some other data corroborate them.

A non-migrated radargram and its interpreted section are shown by [18] to characterize TDS and foredunes ridges in the Quinta-Cassino strandplain. That GPR survey line (Figure 6 in [18]) was carried out upon an NNE elongated TDS covering the footwall block in the limit between Ridges Set 4 and 5. However, that

[2]The authors invited [18] for GPR data exchange and sections for GPR data processing (migration) to a common publication. But, until nowadays, no answer was received. The doors remain open to file exchange.

non-migrated radargram presents a series of diffraction hyperboles and hyperboles interference pattern, most of them concentrated in the swale's areas and in the inner part of crests. There is also a series of bow-tie interferences in the swale's areas. The "X" pattern of diffraction tails interference in the inner part of crests cannot be taken as due to cross-stratification of wind-formed dunes. In fact, the diffractions and their interference patterns obliterated some of the reflections continuity in the non-migrated radargram and introduced artifact pitfalls as discussed before.

**Figure 7** offers a preliminary re-appreciation for that non-migrated radargram (Figure 6 in [18]). A careful examination in that radargram shows that most of the seaward dipping reflections can be followed into the upper radarfacies composed by arcuated crest, even though the presence of minor diffraction hyperboles truncations. The pattern that emerges is a series of reflections climbing the lower ones, which is not due to the wind-formed structures. These re-interpretated radarfacies signature is completely compatible with that recorded in Danube Delta [39]. The reflections continuity, even in a non-migrated radargram, shows that it is possible to interpret them as beach-ridges.

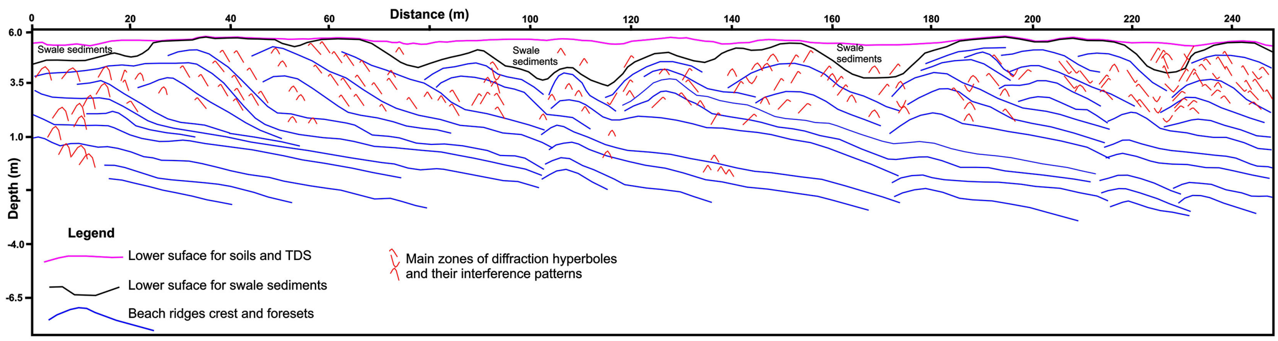


**Figure 7.** Re-interpretation of the non-migrated radargram (Figure 6(B) in [18]) showing diffraction hyperboles and interference patterns truncating the continuity mainly in beach ridges crest and swale zones. See text for discussion. That radargram is placed parallel to SPT profile and close to SPT_4 identified in **Figure 2**.

Another radargram shown by [18] should receive attention (**Figure 8(A)**). In that radargram, the effect of diffraction hyperboles on geological structures is also observed in the tips of the Pleistocene-Holocene interface reflector, primarily at radargram coordinates (~300, −1) and (~400, −14). These tips show high reflectivity and are the convex (upper, in the footwall) and concave (lower, in the hangingwall) points for wave diffraction related to normal fault [36] [37]. These are classical, well-known structural features that produce diffraction hyperboles and strong interference patterns (artifacts pitfall). Toward SE, three others of such features can be recognized: at ~800 m, ~1150 m and ~1500 m.

It is possible to observe (**Figure 8(A)**) that both the Pleistocene-Holocene interface faulted reflectors on the left radargram side are gently dipping landward (NW). This is a well-documented feature of rotational faults developed in the gravity sliding tectonic blocks [25] [26]. Counterclockwise block rotation in

RGSCP was already presented [6] [9].

Figure 8(B) also offers a new alternative interpretation for [18] radargram despite its strong diffraction interference pattern. The picture emerging from a non-migrated radargram is clear to someone familiar with geophysical data processing. In this way, it can be concluded that SPT-9 was drilled in a horst structure.

Comparing Figure 8(A) and Figure 8(B), one can follow the Pleistocene-Holocene interface from northwestern lower hangingwall position (where it is a high amplitude reflector) toward ~750 m SE, where there exists another zone of high diffraction interference. From ~800 to 950 m and 1000 to ~1175 m SE, the Pleistocene-Holocene interface is horizontal; but, at ~1175 m, a new diffraction zone interrupts it. And, from ~1375 m to ~1500 m SE, this same reflector is well distinguished, gently arcuated, to be projected toward northwest against the diffraction zone (a fault plane displaying small vertical slip).

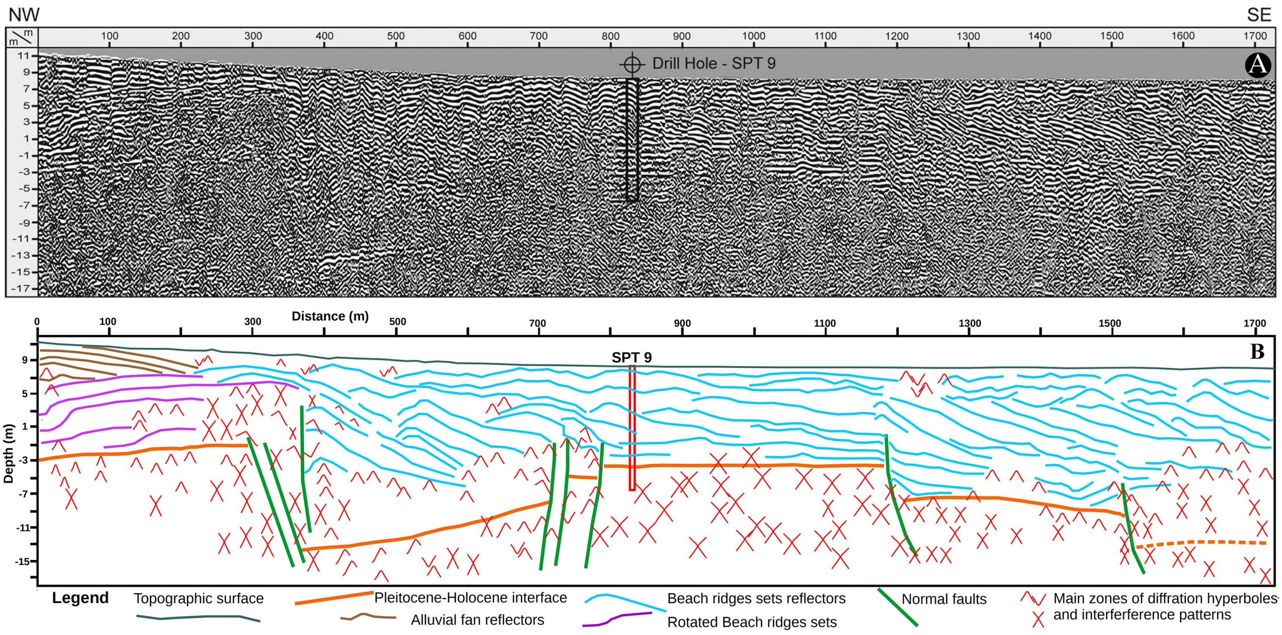


Figure 8. Evidence for normal fault blocks in the Quinta-Cassino strandplain. (A) Radargram from Figure 7(A) in [18] (used with @Elsevier permission). (B) Re-interpretation of the radargram considering Pleistocene-Holocene contact truncated by diffraction hyperboles and interference patterns zones located mainly in downthrough fault blocks and beach ridges crests. See text for discussion. This radargram is placed nearly orthogonal to Quinta Main Listric Fault outside to the south of the area shown in Figure 2.

Additionally, in the NW major fault plane, the upper (footwall) and lower (hangingwall) tip points of the Pleistocene-Holocene interface (Figure 8(A)) are the sources for diffraction and interferences, giving rise to a zone displaying "X", "Λ" and "V"s (diffraction hyperboles interferences). The upper limit of this structure is placed in an oceanward-dipping reflector where the interference intensity vanishes; it was interpreted as a ravinement surface [18], but it best characterizes the oceanward foresets of beach ridges.

The inner reflections for radarfacies interpreted by [18] show a random/chaotic distribution in its base and gradually change to inverted "V"s close to the upper limit (**Figure 8(A)**). It was interpreted as estuarine/lagoonal facies [18]. However, they do not have any resemblance to well-developed configuration and continuity of the estuarine and lacustrine/lagoonal reflections (e.g., [40]).

The faulted Pleistocene-Holocene contact geometry, as interpreted in **Figure 8(B)**, is in accordance with fault blocks displacement in extensional segment of the gravity sliding blocks [6] [9] [10] [25] [26]. This geometry is also in accordance with the domino-like geometry of the Pleistocene substrate shown in Quinta-Cassino strandplain geological section ([18], see their Figure 4).

**Figure 8(B)** demonstrates that a horst-type structure is suitable for the Pleistocene basement in the Quinta-Cassino strandplain area. The non-migrated radargram leaves several diffraction hyperboles and their interference patterns masking sedimentary structures and fault planes.

The re-interpreted radargram (**Figure 8(B)**) enables a comparison with SPT drillholes section (**Figure 9(A)**) and radargrams due to ([6], especially their Figure 7), even though it is located SSW from that SPT drillhole section. The structural architecture of a subsiding hangingwall fault block due to gravity sliding varies along strike but still can show some similar features in different sizes. Considering the published radargrams in the Quinta-Cassino area [6] [18] and the re-interpreted one (**Figure 8(B)**), and the SPT drillhole section due to [18], it is possible to investigate fault vertical slip and look for differences and similarities in displacement pattern. Such evaluation can help in a better understanding of Quinta-Cassino strandplain and in its development.

The geological section presented by [18] shows that SPT-0 and SPT-1 (**Figure 9(A)**) are located very close to radargrams presented by [6] (see their Figure 7). Then, it can be easily seen that SPT-0 [18] is placed westward of the Quinta Main Listric Fault escarpment (in fault footwall), while the SPT-1 is placed eastward (in fault hangingwall). The height difference for Pleistocene basement in the geological section (**Figure 9(A)**) is ~12.5 m. This difference is close to down-dip slip of the hangingwall block as shown in radargram (Figure 7 in [6]): ~12.0 m.

An examination on other radargrams (Figures 6-8 in [6]) shows that down-dip slip of the hangingwall fault block in the Quinta Main Listric Fault escarpment has a small range of values (9 - 15 m). This down-dip slip range is to be taken as the depth difference between the Pleistocene upper boundary in the footwall (westward of escarpment) and in the hangingwall (eastward of escarpment).

The agreement between down-dip fault slip and height difference for Pleistocene basement in geological section (**Figure 9(A)**) is in accordance with their proximity to the >60 km long Quinta Main Listric Fault. Anyway, down-dip slip is expected to vary along the gravity normal fault and vanish toward its lateral tip zones, or even in small fault hangingwall blocks that could exist.

Radargrams presented by ([6], in Figures 9-11) were located to investigate the limit between beach ridges sets 1, 2 and 3. These radargrams show that Pleistocene-Holocene interface is at 15 to 20 m depth. The SPT-2 and SPT-3 drilled by [18] show that the depth to the Pleistocene-Holocene interface is respectively 15 and

20 m. Even that radargrams were surveyed > 3 km far from SPT drillholes, careful observation of radargrams [6] and geological section (**Figure 9(A)**) shows that they are all in accordance. It is still to be noticed that SPT-2 is close to the limit between beach ridges set 1 and 2, while SPT-3 is closer to beach ridges set 4. The stair-like geometry of the Pleistocene-Holocene interface shown in the geological section (SPT-0, SPT-1, SPT-2 and SPT-3) presented by [18] can be easily understood if the down-dip slip developed in this key interface by radargram's normal faults is observed [6].

The above re-interpreted radargram (**Figure 8(B)**) shows a vertical fault slip ~13 m for its westernmost normal fault. The original radargram (**Figure 8(A)**) was surveyed to the south, approximately to the midway point regarding the Quinta Main Listric Fault escarpment. Unfortunately, this radargram did not begin upon the Pleistocene Barrier III, and the Quinta Main Listric Fault could not be identified. This hidden fault is far from beach ridges sets 1 and 2 limit and tells that normal faulting in the area developed minor and major diachronic displacements. The corresponding geological section (Figure 5 in [18]) shows that Pleistocene-Holocene limit was only recognized in the northwesternmost drillhole (SPT-9), and was not identified in the drillholes toward SE, even they were drilled deeper. The reason may be the increasing in down-dip normal fault slip toward SE.

**Figure 7** and **Figure 8** show that non-migrated radargrams introduced biased interpretations, due to un-removed (non-collapsed) diffraction hyperboles (artifact pitfalls) which obliterate the reflection on geological features. The re-interpreted radargrams (**Figure 7** and **Figure 8**) analysis and discussion, despite the previous interpretation [18], put important clues in foredune ridges hypothesis in the Quinta-Cassino strandplain. The detailed geomorphic investigation due to [14], the geophysical data due to [6], the geochronological data [14] [18] and the re-interpreted radargrams (**Figure 7** and **Figure 8**) led to the following conclusions:

1) Transgressive dune/sand sheets (TDS) do not cover beach ridges completely. In other words, it can be easily seen (aerial photographs, satellite images, Google Earth images) that sand sheets transgressively and partially drown a previous linear structure (the beach ridges) as previously described by [16]. A careful examination of images shown in [14] and [18] demonstrates that this geomorphic feature is observed.

2) The seaward younging TDS are mostly aligned upon the trace lines dividing each beach ridges set [14] [18]. In the Quinta-Cassino strandplain, landward far from dunefield at actual beach, the TDS still covers the previous ridges. In these positions, TDS is wider than ridges and is aligned with those dividing lines. But TDS is not a widespread geomorphic feature covering the long ridges in the strandplain area.

3) These results indicate that each trace line separating beach ridges sets is a splaying and bending listric normal fault, and TDS are mainly developed in the

footwall block. Despite the minor splayed and bended normal fault, the strandplain hangingwall block does not show the same topographic amplitude as the Quinta Main Listric Fault escarpment, the vertical displacements are enough for sand blowing from beach to be deposited in the low relief scarps and on the footwall summit at each faulting age.

4) The ridges truncation along trace line separating sets in the north segment and in the southern segment can be well explained by differential normal fault movements. The alternating ridge truncation at trace line separating each ridges set can be a major result of different displacement rates and amounts for the evolving bending and splaying faults. In such a gravity tectonic scenario, ridge truncation cannot be attributed completely to coastal erosion, despite some erosion can be claimed to occur.

5) [14] and [18] did not sample the same material for surficial OSL dating. But superposing that data by their sampling location, the OSL age consistently decreases seaward, showing that TDS are abandoned while ridges prograde toward east. A new TDS is formed when a new splayed and bended normal fault emerges in the surface.

Based on the above analysis and discussion, it is possible to locate a normal fault emerging in each trace separating beach ridges sets. In this way, the careful beach-ridges sets distinction carried out by [14] is in accordance with faults identified in radargrams from [7] and can be used to locate such minor fault splays and bends. The area between the splayed and bended faults is minor fault block in the entire subsiding hangingwall block of the Quinta Main Listric Fault.

These evaluations do permit to elaborate a re-interpreted geological section for SPT drillholes and geochronological data from [18] but also including geochronological and geomorphic data from [14] and location of radargrams. This re-interpreted geological section is presented in **Figure 9(B)** to discuss the geological evolution of Quinta-Cassino strandplain.

**Figure 9(B)** considers, then, that the Holocene sandy radarfacies interpreted by [18], below heavy minerals (HM) records, are, in fact, the same sedimentary unit (the linear beach ridges well visible in images) covered, in some places, by TDSs. The geological element to distinguish between TDS/TD and beach ridges sands is the presence of heavy minerals lamination. The architecture of beach ridges reflectors in re-interpreted radargrams (**Figure 7** and **Figure 8**), radargrams presented by [6] and vertical normal fault displacements as earlier discussed are applied to re-interpret the entire SPT drillholes section (**Figure 9(A)**).

The listric faults were placed where the ridges' set limits were identified according [14]. The Pleistocene-Holocene interface was set according to initial discussion about gravity tectonics, fault geometry, block rotation, existence of horst structures, and known vertical fault displacement. The introduction of normal faults and their displacements (as discussed earlier) makes it possible for the geological correlation between SPT drillholes to consider the geochronological data and the vertical time span for each drillhole in each fault block.

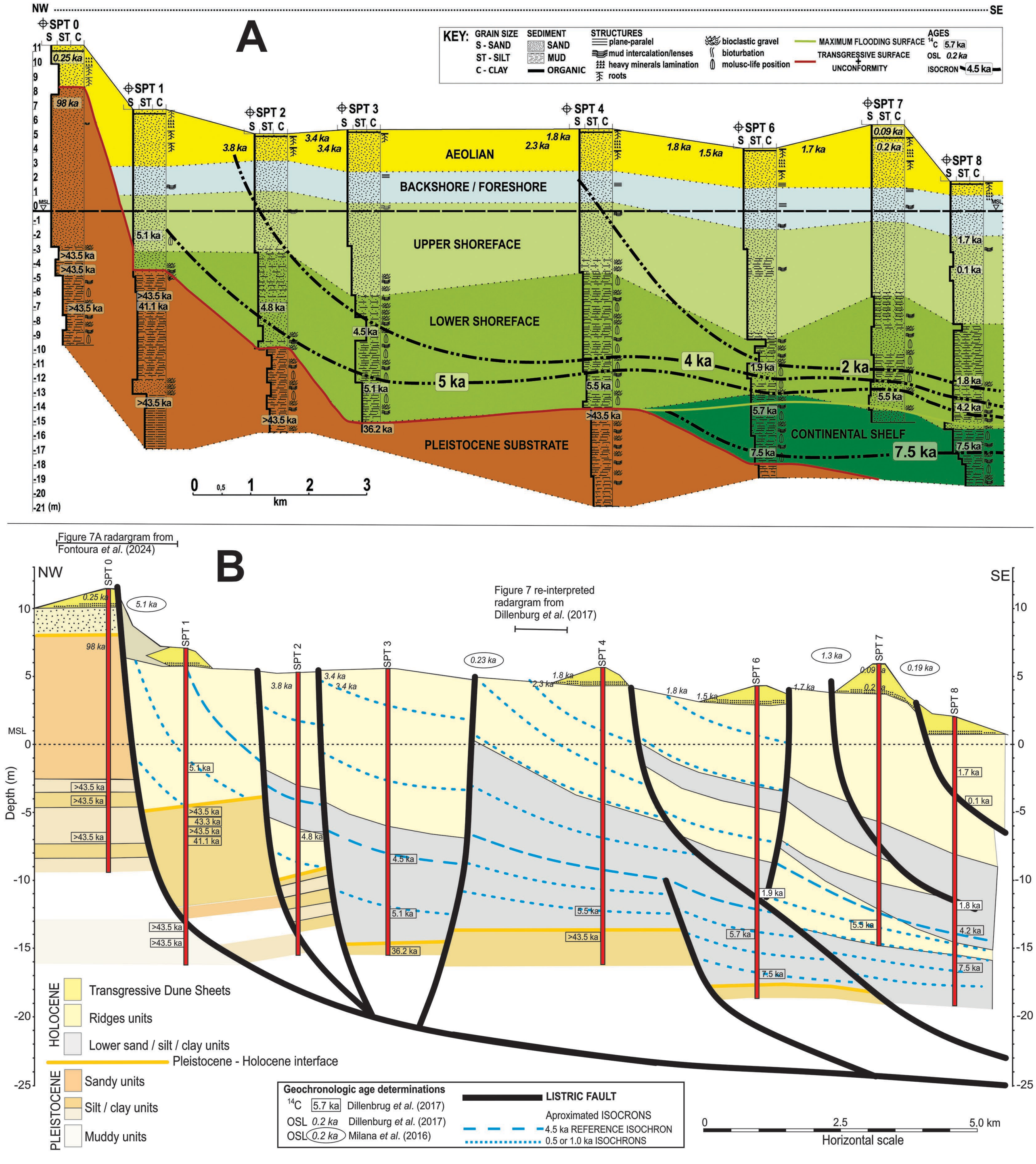


**Figure 9.** A geological cross-section in the north sector of the Quinta-Cassino strandplain. (A) The previous geological section (Figure 4 in [18], used with @Elsevier permission). (B) The re-interpreted cross-section with data from [6] [14] [16] [18] showing the listric fault development and sedimentation in the Quinta-Cassino strandplain. The surface topography in re-interpreted cross-section (B) was computed in Google Earth. See text for discussion.

These procedures did permit tracing isochrons in each fault block, taking into account age data in corresponding SPT, which enables to realize that each one has a different sedimentation rate. A 4.5 ka isochron is placed for reference, and 0.5

or 1.0 ka isochrons are also drawn considering the ages determined in each drillhole [18] or in surface sands [14] [18]. A close examination of sampled sites showed that some ages were determined in recently remobilized TDS, not exactly in beach ridges materials or in older TDS. The sedimentation rate in each SPT can then be easily approximated using depth and age differences.

The re-interpreted geological section model (**Figure 9(B)**), then, shows more reliable isochrons for each fault block. This re-evaluation accounts for a more regularized accumulation rate of sedimentation in the Quinta-Cassino strandplain and shows that each fault block can have a different accumulation rate according to the faulting development. It also puts in evidence that older and finer-grained sediments (SE drillholes) seem to have a lower sedimentation rate than the upper sandy units (beach ridges).

The most interesting aspect of the initial geological section presented by [18], however, is the sedimentation rate. Considering the determined ages [18], the vertical accumulation rates can be estimated from 7.5 to 10.0 mm/y in the northwestern drillholes, up to 100.0 mm/y in SPT-8. The beach ridges propagation rate in the Quinta-Cassino strandplain was carefully constrained by [14]: taking RG1 OSL age (5110 yr) close to Quinta Main Listric Fault to RG4 OSL age (190 yr), the horizontal progradation of the strandplain is ~3.56 m/y (~17,500 m distance).

Aeolian processes usually have vertical accumulation rates varying from 0.1 to 1.0 mm/y (e.g., [41]-[44]) constructed the chronology of progradation for three Holocene coastal sand ridge plains in southeastern Australia. [44] found a horizontal progradation rate ~0.3 m/yr for Moruya and Wonboyn beaches, and a progradation rate ~0.1 m/yr for Callala Beach.

The vertical accumulation rates for estuarine environment, on the other hand, show a range of values: from 0.3 - 0.9 mm/y to 27 - 70 mm/y, depending on sediment supply, position in the estuary, and coastal wide [45]. [46] also determined a vertical sedimentation rate in the range of 1.7 - 2.3 mm/y in Niger Delta passive continental margin.

Based on vertical sediment accumulation rates data gathered from past ~ 55 years of peer-reviewed literature, [47] applied a machine learning-based Global Predictive Seabed Model (GPSM) to produce a 5-arc-minute global map of predicted benthic vertical sediment accumulation rates. In the RS coast (Brazil), this model [47] predicts vertical sedimentation rates to 20 - 30 mm/y and a standard deviation between 2.5 to 10.0 mm/y for that prediction.

The vertical sediment accumulation rates and the eastward (horizontal) progradation in the Quinta-Cassino strandplain fit better with estuarine and marine rates than to aeolian processes rates. This makes clear that the local mechanical subsidence due to identified faults accounts for accommodation space in the Quinta-Cassino strandplain extending southward (from Rio Grande to Sarita area).

## 5. Discussions on the Holocene Structural Evolution of the RGRZ

The recently identified Holocene gravity sliding normal faults [5]-[9] of the

RGSCP were developed in the shallow segment of the Pelotas Basin [19] [20]. It was demonstrated that this gravity sliding tectonics (not to be confused with thick-skinned rifting) controlled most of the Holocene sedimentary unit's deposition in the RGSCP. **Figure 10** shows the regional setting for these structures and lights the main structural difference between the Bujuru and Rio Grande relay zones. Basic nomenclature for normal faults and related structures can be found in [48], which can be applied either in thick-skinned or in thin-skinned normal fault tectonics.

The Bujuru Relay Zone, at southern Lagoa do Peixe Listric Growth Fault [7] and northern Retiro-Estreito Main Fault [8], is a structural high (mainly an anticline) of Pleistocene sedimentary units that was the primary structural barrier for the younger Holocene sedimentary barrier (TD and TDS). The Bujuru relay zone shows poor fault splaying and bending in the tips for both normal faults [7] [8].

The Rio Grande Relay Zone (RGRZ, **Figure 10(B)**) shows strong splaying and fault bending in the Quinta Main Listric Fault's northern tip [6] and in the southern tip for Retiro-Estreito Main Fault [9]. The tips for both faults seem to show interacting [49] or even crosscutting relationships. To better solve these relationships, careful and guided geophysical surveys have been carried out (e.g., [5]-[9]), surveying deeper than has usually been done, taking into account the TDS and TD Holocene covers.

It is to be realized that, in the Lagoa do Peixe Listric Growth Fault [7], the hangingwall strain is mainly taken up by the continuous folding above the listric fault surface. On the other hand, in the southern tip of Retiro-Estreito Fault and northern tip of Quinta Main Listric Fault, strain is completely partitioned into several subsidiary faults that branch off the main listric fault (splays, imbricate fans, or segmented fault arrays). In this last case (RGRZ), the subsidiary fault displacements are episodic, diachronic and recurrent to build up the local subsidence.

The Rio Grande structural High [19] plays an important role in Quinta Main Listric Fault (**Figure 3(B)**). The shallow Pelotas Basin crystalline basement tilt during the regional flexural subsidence stage is one of the most important triggering mechanisms for the gravity sliding tectonics in the RGSCP, while the differential sedimentary loading and compaction around Rio Grande structural high could certainly induce and control the listric normal fault splaying and bending. Such structural highs can act as mechanical buttresses and local stress concentrators, which force normal faults to branch, to change their strike and/or dip angles, and even to invert to produce antithetic faults (e.g., [50] [51]).

The Rio Grande Relay Zone (RGRZ) is not actually a Pleistocene structural high (**Figure 10(B)**), as could be recognized in the Bujuru Relay Zone [7]. The initial stages of the RGRZ, during Quinta Main Listric and Retiro-Estreito fault tips propagation and approximation, showed un-faulted Pleistocene units at higher level positions (10 - 15 m above m.s.l.). However, the fault tips propagation, juxtaposition and interaction, chiefly due to the sequential splaying and bending of subsidiary faults to Quinta Main Listric Fault, leading to the production of a depressed area, successively filled with Holocene sediments to build up the Quinta-Cassino strandplain.

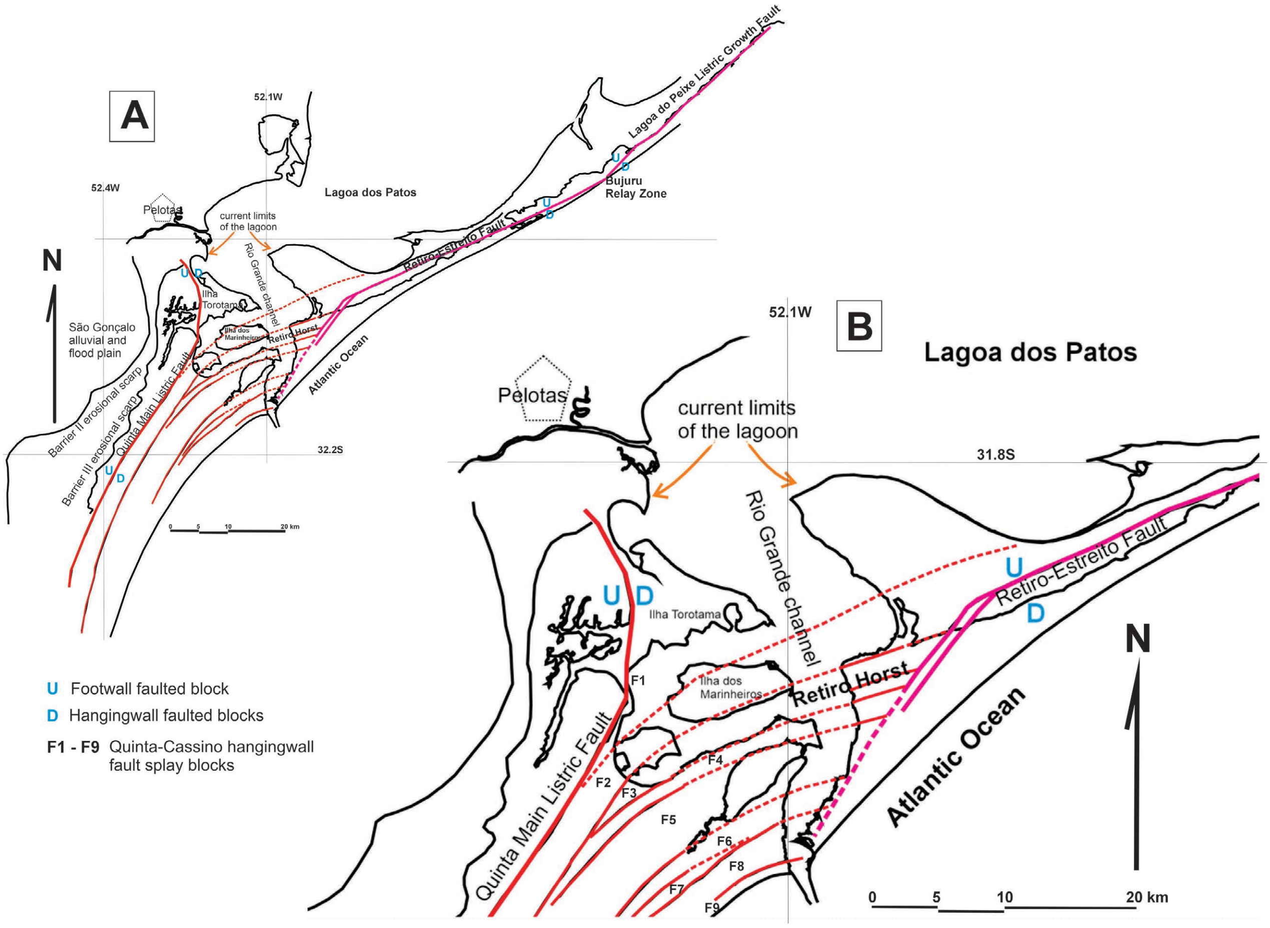


**Figure 10.** Regional structural framework of the RGSCP, showing the main gravity sliding normal faults controlling Holocene sedimentation. (A) The regional middle to southern RGSCP structures. (B) Detail structural map in the RGRZ, illustrating the fault blocks (F1 - F9) in the Quinta-Cassino strandplain.

**Figure 11** shows the final structural evolution of faulted Pleistocene units (basement for Holocene units). It is to be realized that Pleistocene basement for Holocene subsided area in the RGRZ is, at the first deformational stage, the footwall for Retiro-Estreito Main Fault, since the Quinta Main Listric Fault had not propagated yet to the north to develop the interaction structure.

The splaying and bending of the subsidiary normal faults of Quinta Main Listric Fault would interact with the footwall block of the Retiro-Estreito Main Fault in the evolving time. This kind of interaction produced the relay ramps and transfer zones in the northern limit against the Retiro-Estreito Main Fault. The identified Retiro Horst [9] can be taken as the northern limit of a relay ramp. The Ilha dos Marinheiros must have also remained as a structurally elevated block (a secondary horst) in this scenario.

**Figure 10(B)** and **Figure 11** show the limits for splay fault blocks from Quinta Main Listric Fault (F1 to F9), as already characterized in the previous section.

They do reflect the beach ridges sets first identified by [16] and are in accordance with faults identified in radargrams discussed in the previous section and **Figure 9(B)**.

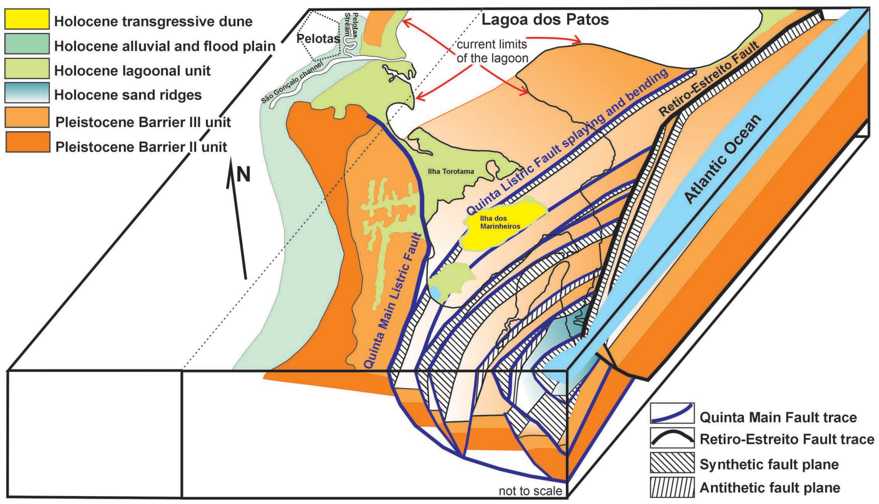


**Figure 11.** Block-diagram illustrating the Quinta Main Listric Fault splaying and bending and its interaction with Retiro-Estreito Main Faults to give rise to the Rio Grande Relay Zone, and the asymmetric Quinta-Cassino strandplain. Holocene sedimentary units, except someone's for reference, were omitted to highlight basement (Pleistocene) structural features. Gradient colouring in plain view for upper Pleistocene unit represent deeper (light) to higher (dark colour) structural levels in relay ramps.

[14] produced a careful map, numbering each individual beach ridge in the Holocene Quinta-Cassino strandplain and distinguished 18 sets of coastal ridges, based on ridges lineaments truncation, ridges topographic altitude and ridges erosion evidence. [14] suggested 5 stages of ridges formation due to different conditions of longshore sediment transport, wind intensity and sediment. Unfortunately, [14] did not have geophysical data at that time to recognize the normal faults as recently done [6]. In anyway, the 18 ridges set characterized by [14] could be exactly regrouped into the subsidiary fault blocks (F1 to F9) using the defined lines of truncation. This first approach in defining the fault blocks does not mean that each of the 18 sets previously defined [14] is not fault-related, as could be envisaged from the discussion in **Figure 8**. It only means that, for the actual data and surveys results, it is better to constrain the structural evaluation. Furthermore, it is to keep in mind that normal fault splays show diachronic and recurrent displacements, which can account for major and minor ridges lineaments truncation and ridges topographic altitude.

The evolution of the Quinta-Cassino strandplain should then be evaluated based on structural criteria, namely those regarding fault splaying [52], fault tip propagation, fault overlapping and fault interaction [53]-[57]. Again, this statement does not mean that environmental variables such as sediment supply, inlet migration and coastal hydrodynamics do not contribute with beach ridges formation. It only means that mechanical subsidence (fault-related subsidence) had played a greater role in Quinta-Cassino strandplain development than other environmental conditions. This observation can be followed from previous discussion that vertical accumulation and horizontal progradation rates for Quinta-Cassino strandplain are much higher than those for aeolian processes and stands in the upper limit for estuarine environment.

The Quinta Main Listric Fault and its subsidiary splays tip propagation toward the north and also the southward propagation of the Retiro-Estreito Fault tip led to the formation of an initial structural high in the RGRZ. Figure 12(A) illustrates this initial stage, where mechanically subsided areas are located only close to both fault scarps. It should be remained that, at tip zone of each normal fault, the vertical displacements tend to zero. In this way, the footwall for Retiro-Estreito Main Fault was progressively faulted to be the hangingwall for Quinta Main Listric Fault.

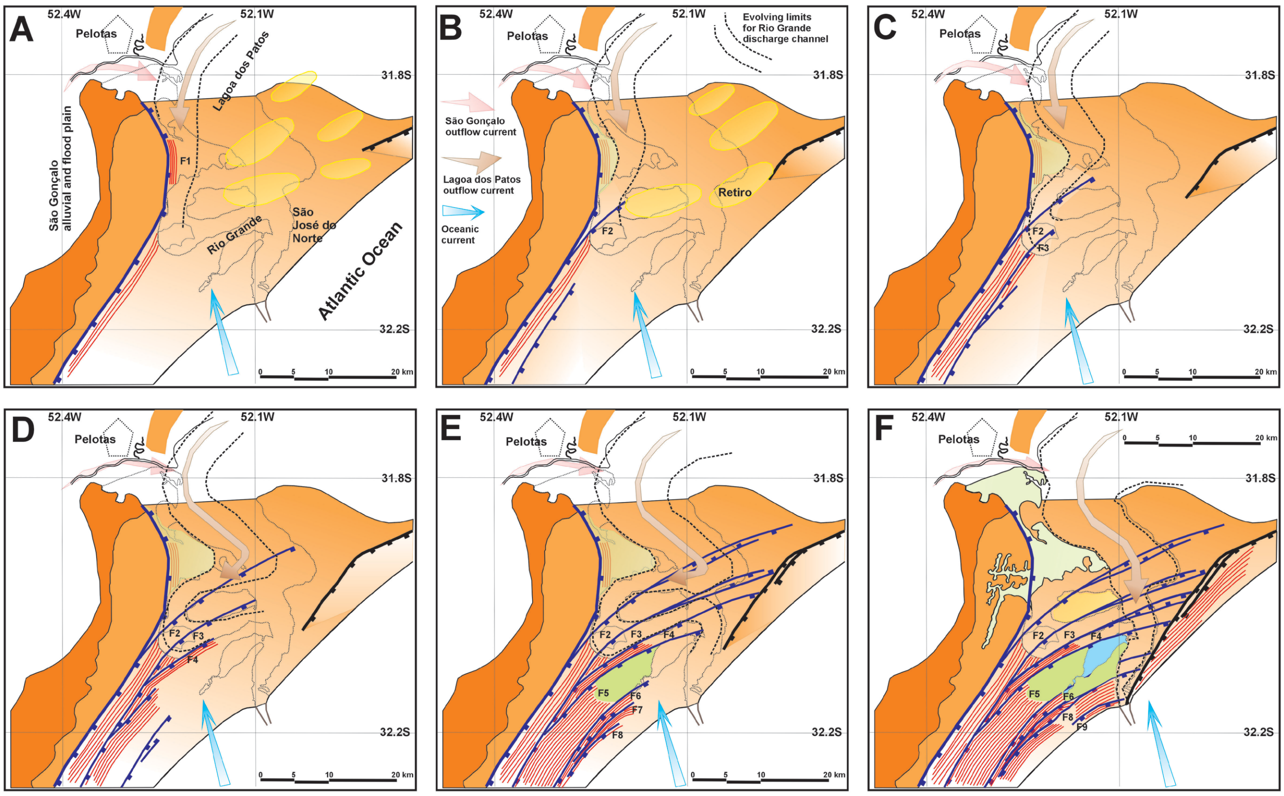


**Figure 12.** Illustration of the Rio Grande Relay Zone structural and sedimentary evolution during the Holocene, focusing on asymmetric Quinta-Cassino strandplain development. (A) - (C) Fault propagation stages without splays overlapping into Retiro-Estreito Fault. (D) Splay faults overlapping stage into Retiro-Estreito Fault. (E) (F) Splay faults interaction stage into Retiro-Estreito Fault.

The splaying sequence and displacement for listric fault and their propagation against the footwall of the Retiro-Estreito Main Fault progressively constrained the RGRZ structural high in the Retiro area (São José do Norte). The northward propagation of the Quinta Listric splay faults against the Retiro-Estreito Fault footwall progressively increased the local mechanically depressed area in the Quinta-

Cassino. This wedge-like mechanically subsided area (map view) in the Quinta-Cassino controlled the sedimentation shouldered against the Quinta Main Listric Fault and the relay ramps of the Retiro-Estreito Main Fault footwall (**Figures 12(A)-(F)**).

The westernmost fault block (F1) represents a remnant of the unfaulted Quinta Main Listric Fault hangingwall in the initial stages of the listric fault development (**Figure 12(A)**). The beach ridges are still distinguished in Ilha Torotama, overlaid by actual lagoonal sediments [6]. To the south of Quinta district, the substage 1a [14] ridges lineaments may also be regarded to F1 fault block. The high truncation angle for these beach ridges lineaments (#1 - #36) against the Quinta Main Listric Fault scarp is due to main fault bending toward NNW and its high total vertical fault downthrown displacement.

[14] estimated, based on OSL date for numbered ridges lineaments, 5899 yrs BP as the start age for beach ridges formation in the Quinta-Cassino strandplain. **Figure 9** shows that the oldest Holocene sediment is placed in SPT6, and sequentially in SPT4 and SPT1. This sequence points that the Quinta Main Listric Fault propagated toward west, and emerged as a fault scarp ~6.0 ka, giving rise to the initial mechanically subsided zone in the Quinta-Cassino strandplain.

The differential mechanical subsidence in the Quinta Main Listric Fault hangingwall (downthrown block) and the elevated footwall block of the Retiro-Estreito Fault makes possible the Lagoa dos Patos channel discharging firstly parallel or at a very low angle to the Quinta Main Fault (**Figure 11** and **Figure 12(A)**). At the first stage of Quinta Main Listric Fault and Retiro-Estreito Fault approximation (not still overlapping), the large and elevated block at north (Retiro area) acted as a structural barrier against which the deltaic plain was initially built up (**Figure 12(A)**).

The initially narrow subsided hangingwall of the Quinta Main Listric Fault channelized the Lagoa dos Patos discharge close to Quinta Fault scarp (**Figure 12(A)**). The erosion of Pleistocene sedimentary units standing in higher structural levels (up-stream Lagoa dos Patos and São Gonçalo floodplain) should have provided sediments for the prograding beach ridges system in the Quinta-Cassino strandplain.

[16] and [17] previously proposed that Lagoa dos Patos channel was initially close to the Quinta Escarpment (**Figure 12**). "*The presence of these beach crest structures* [beach ridges set 1], *and the Pleistocene Barrier III show that the current access communication between the Lagoa dos Patos and the Atlantic Ocean was made through another location*" [16]. "*It was located in the southernmost part of the area* [the northwestern corner of the wedge-like tectonically depressed Quinta-Cassino area], *going around the Ilha dos Marinheiros, which was part of Barrier III, and flowing south of the Cassino beach area*" [16].

[16] pointed out that the first beach-ridges set (F1) "*shows a concavity towards the mainland, testimony to a relatively low depositional energy due to the wide opening of the estuary*". These environmental conditions could have operated at

~6.0 ka, while the Quinta Main Listric Fault propagation in that area has not yet produced significantly high episodic subsidence. In this scenario, the estuary was initially open to the south, and the initial energy flux and sediments transport from upstream the Lagoa dos Patos channel may have been low, while the oceanic current is directed against the elevated Quinta footwall faulted block.

The current geological and structural data suggest that Lagoa dos Patos was broadening during the Holocene period (Northgrippian and Meghalayan ages). The splaying and bending faults induced local mechanical subsidence in the widening Quinta-Cassino strandplain and explained the increasing flow and eroding capacity of lagoonal discharges as earlier envisaged by [16].

The following faulted blocks to be displaced are SPT3, SPT2, SPT7 and SPT8. The $^{14}C$ ages determined by [18] along the drillholes suggest diachronic movements in the splaying listric faults related to Quinta Main Listric Fault. It is important to note that fault tip propagation is north to northeast for Quinta Main Listric Fault and is toward south for Retiro-Estreito Fault (**Figures 12(B)-(D)**). Fault overlapping (**Figure 12(C)**, **Figure 12(D)**) may have initiated a period of higher strain partitioning and distribution, implying higher number of fault splays and bends [53]-[57].

The following fault blocks making up the Quinta-Cassino a wider subsiding wedge hangingwall (F2 - F9), each one with its proper beach-ridges sets [14] [16], are "*characterized by a degree of concavity of the different ridges … oriented towards the ocean*, [and] *show that they were formed under the influence of the outflow of lagoon waters in a high-energy environment*" [16]. These environmental conditions are in accordance with recorded increasing vertical sedimentation rates from SPT1 to SPT8 [18] and are seen in **Figure 9(B)**. These environmental conditions operated while the Quinta-Cassino depressed area was being widened by fault splays propagation (**Figures 12(B)-(D)**), but mainly when the Quinta Main Listric Fault and Retiro-Estreito Fault initiated the overlapping and interaction (**Figures 12(D)-(F)**). The Quinta splay listric faults bending, however, should also have played some control on the beach-ridges sets development.

[17], based on a high-resolution seismic (near-surface) survey, recognized a sequence displaying tangential reflections pattern (downlap to the base), which was interpreted as a "*succession of coastal ridges*". It is to note that this seismic line was surveyed in the new Rio Grande Harbor (**Figure 2**), following the fault block F4 continuation (**Figure 10**, **Figures 12(D)-(F)**), but they are almost completely drowned by current lagoonal, TDSs and coastal dunefield (TD). This record shows that beach ridges were deposited against the Retiro-Estreito elevated footwall block, forcing the Rio Grande channel to meander around Ilha dos Marinheiros during the initial stages of splay faults overlapping the Retiro-Estreito Fault. According to [17], at this period, "*the depositional conditions were characterized by a high availability or input of sandy material. … indicative of a high transport energy and is comparable to several regressive progradation coastal models*". Additionally, the oceanic currents were strong enough to make beach ridges prograde NNE at

this stage.

[9] showed the Retiro Horst as a local structural high, separating diverging beach ridges patterns (**MR-$f_{n+2}$-br** radarfacies): foresets toward west and east on each horst side. This pattern indicates that oceanic currents accessed the Retiro area from the Quinta-Cassino strandplain and from an eastern position. [9] also showed that beach ridges radarfacies is covered by backshore and washover deposits (**MR-$f_{n+3}$-bf** radarfacies), which suggests the initial stage of Retiro Horst rupture do give rise to the actual Ilha dos Marinheiros.

The structural and environmental conditions, then, show that the complete rupture of the splay fault block F2 to isolate the Ilha dos Marinheiros and to define actual Rio Grande flow channel is mainly due to the faults overlapping and interaction (**Figures 12(D)-(F)**). This episode may be related to another increase in sedimentation rate (SPT7, SPT8, **Figure 9**).

**Figure 12** shows, then, how an asymmetric delta was being constructed and the gravity sliding gave rise to a wedge-like depression for Quinta-Cassino strandplain deposition.

The gravity tectonics, as pointed out by [26] [27] [29] [30] [58] [59], often redistributes previously deposited sediments. Then, the erosion of Pleistocene sedimentary units, upstream to Lagoa dos Patos and São Gonçalo floodplain, must have supplied the enough sand and clay material to build up the strandplain beach ridges. A close observation in the northern segment of the Quinta Main Fault (from Quinta to Torotama, **Figure 11**) shows that Pleistocene Barrier III is under erosion in its eastern side (Fault escarpment) and its western side (erosional terrace). The same re-entrant erosional pattern upon Pleistocene Barrier III is observed in both margins of the Lagoa dos Patos [7]-[9]. Then, it could be realized that two limits for Pleistocene Barrier III exist: 1) a rectilinear to curvi-rectilinear one (fault-controlled) and 2) a re-entrant (drainage-controlled) one, which is characterized as an erosional terrace.

## 6. Conclusions

The Rio Grande Relay Zone is a complex structural area developed in the shallow Pelotas Basin due to basement tilt during the regional flexural basin subsidence stage. The regional flexural subsidence, basin scale, is the triggering mechanism for gravity sliding process in onshore (RGSCP) and offshore shallow Pelotas Basin, but also in the deep Pelotas Basin (Rio Grande Cone, continental platform, slope and rise).

The Rio Grande Relay Zone is defined by the interaction of the Quinta Main Listric and Retiro-Estreito splaying and bending faults tips. The geometry of this relay zone is influenced by the differential sedimentary loading and compaction around the Rio Grande Structural High.

The Rio Grande Relay Zone developed from a structural high (footwall for Retiro-Estreito Main Fault) to a local mechanically subsided area due to the interaction of the hangingwall block of Quinta Main Listric Fault (Quinta-Cassino) against the footwall block of the Retiro-Estreito Main Fault. The wedge-like depressed area (map view), then, gave rise to an asymmetric delta, the Quinta-Cassino strandplain, whose discharging channel meandered close to the Retiro-Estreito Main Fault footwall and the relay ramps of the RGRZ. The episodic and diachronic local fault subsidence developed conditions for "*high availability of sandy material*" and also "*high transport energy*".

Recent studies [5]-[9] show a wide role of evidence for gravity sliding tectonics in the RGSCP. [4] previously reviewed and evaluated several local publications reporting neotectonic activity. [4] also regarded the Mangueira Lineament and Lagoa do Peixe Lineament as probable faults and suggested a geophysical survey to investigate them. Fortunately, [5]-[9] could carry out such a geophysical survey to highlight that the previously named Quinta and Lagoa do Peixe escarpment, usually taken as a linear erosional feature, are in fact the Quinta Main Listric Fault and Lagoa do Peixe Listric Growth Fault. Additionally, Retiro-Estreito Main Fault was also identified and characterized [8] [9]. These results show that a series of geomorphic evidence was previously presented [4], but the complementary investigations were not carried out, or that evidence was misevaluated.

It is recognized that the proposition of new geological models for the development of some areas has strong impact on the scientific community, even some clues had been presented for a long time. It is to consider that the gravity sliding tectonic imprints in the RGS Coastal Plain were not considered for more than 45 years, even though presented evidence. Then, a great effort is being carried out dealing with several structural data, seismic and GPR sections, and geological mapping to cover the many remaining gaps.

It was demonstrated that questions may be argued on un-migrated radargrams, especially those produced by unshielded and not well-grounded antennas, due to high incidence of surface and subsurface diffraction hyperboles.

It was also demonstrated that the progradation rate for the Quinta-Cassino strandplain is ~3.5 m/y and fits better to estuarine processes than to aeolian ones (foredune interpretation [18]). The vertical accumulation rate also fits much better to estuarine processes: 7.5 to 10.0 mm/y in the northwestern drillholes, up to 100.0 mm/y in southeast ones.

The main conclusion at all is that Holocene lagoon-barrier system in the central to south RGSCP (both sides of Rio Grande High) is fault-controlled. It is also recommended that GPR survey processing procedures apply migration in order to collapse any kind of diffraction hyperboles, but also to position correctly the main reflectors.

## Acknowledgements

B.S.F. thanks to CNPq (Conselho Nacional de Desenvolvimento Científico e Tecnológico) for the Doctoral grant. I.C.S.C. thanks to CNPq for the Productivity Grant (file No. 301634/2022-0) and FAPERGS (Fundação de Amparo à Pesquisa do Estado do Rio Grande do Sul) for the research grant (file No. 24/2551-0001546-9). Authors thank ANP (Agência Nacional de Petróleo), IBGE (Instituto Brasileiro de Geografia e Estatística) and to Bureau Gravimétrique International (BGI: https://bgi.obs-mip.fr/) for making available the geophysical data processed and interpreted in this paper.

## Authors Contributions

**Conceptualization:** Strieder, A.J., Corrêa, I.C.S. and da Fontoura, B.S.

**Methodology:** Strieder, A.J., Corrêa, I.C.S. and da Fontoura, B.S.

**Validation:** Strieder, A.J., Corrêa, I.C.S., da Fontoura, B.S., dos Santos, A.C.O. and Mendes, P.R.

**Formal analysis:** Strieder, A.J., Corrêa, I.C.S., da Fontoura, B.S., dos Santos, A.C.O., Mendes, P.R., Bruch, A.F., Cirolini, A. and Fontoura, J.A.S.

**Investigation:** Strieder, A.J., Corrêa, I.C.S., da Fontoura, B.S., dos Santos, A.C.O., Mendes, P.R., Bruch, A.F., Cirolini, A. and Fontoura, J.A.S.

**Resources:** Strieder, A.J., Corrêa, I.C.S., da Fontoura, B.S., dos Santos, A.C.O., Mendes, P.R., Bruch, A.F. and Cirolini, A.

**Data curation:** Strieder, A.J. and Corrêa, I.C.S.

**Writing:** Strieder, A.J. and Corrêa, I.C.S.

**Writing—review and editing:** Strieder, A.J., Corrêa, I.C.S., da Fontoura, B.S., dos Santos, A.C.O., Mendes, P.R., Bruch, A.F., Cirolini, A. and Fontoura, J.A.S.

**Visualization:** Strieder, A.J., Corrêa, I.C.S. and dos Santos, A.C.O.

**Supervision:** Strieder, A.J. and Corrêa, I.C.S.

**Project administration:** Corrêa, I.C.S. and Strieder, A.J.

**Funding acquisition:** Corrêa, I.C.S.

## Conflicts of Interest

The authors declare no conflicts of interest regarding the publication of this paper.

## References

[1] Alves, E.C. (1977) Estrutura rasa do talude e sopé da Margem Continental do Rio Grande do Sul e Uruguai. Dissertação de Mestrado. Instituto de Geociências, Universidade Federal do Rio Grande do Sul.

[2] Castillo López, L.A., Kazmierczak, T.S. and Chemale Jr., F. (2009) Rio Grande Cone Tectono-Stratigraphic Model, Brazil: Seismic Sequences. *Earth Sciences Research Journal*, **13**, 42-53. http://www.scielo.org.co/scielo.php?script=sci_arttext&pid=S1794-61902009000100004&lng=en&tlng=es

[3] Contreras, J., Zühlke, R., Bowman, S. and Bechstädt, T. (2010) Seismic Stratigraphy and Subsidence Analysis of the Southern Brazilian Margin (Campos, Santos and Pelotas Basins). *Marine and Petroleum Geology*, **27**, 1952-1980. https://doi.org/10.1016/j.marpetgeo.2010.06.007

[4] Fonseca, V.P. (2006) Estudos morfotectonicos aplicados à planície costeira do Rio Grande do Sul e adjacências. Ph.D. Thesis, Universidade Federal do Rio Grande do Sul.

[5] Strieder, A.J., Calliari, L.J., da Fontoura, B.S., Behling, J.S., Wetzel, R.S., Duarte, R.S.S., *et al.* (2015) Gravitational Tectonics Evidences at RGS (Brazil) Coastal Plain Using

Ground Penetrating Radar. 2015 8*th International Workshop on Advanced Ground Penetrating Radar* (*IWAGPR*), Florence, 7-10 July 2015, 1-4. https://doi.org/10.1109/iwagpr.2015.7292667

[6] Fontoura, B.S.d., Strieder, A.J., Corrêa, I.C.S., Mendes, P.R., Bruch, A.F. and Cirolini, A. (2024) Gravity Fault Subsidence and Beach Ridges Progradation in Quinta-Cassino (RS) Coastal Plain, Brazil. *Open Journal of Geology*, **14**, 177-195. https://doi.org/10.4236/ojg.2024.142011

[7] Fontoura, B.S.D., Strieder, A.J., Corrêa, I.C.S. and Mendes, P.R. (2024) Gravity-Driven Listric Growth Fault and Sedimentation in the Lagoa do Peixe, Rio Grande do Sul Coastal Plain, Brazil. *Open Journal of Geology*, **14**, 594-616. https://doi.org/10.4236/ojg.2024.144025

[8] Fontoura, B.S.d., Strieder, A.J., Corrêa, I.C.S., Mendes, P.R. and Nóbrega, A.V. (2024) Structural Controls of the Coastal Bujuru and Retiro Heavy Minerals Deposits in Southern Brazil. *Open Journal of Geology*, **14**, 1016-1037. https://doi.org/10.4236/ojg.2024.1412045

[9] Strieder, A.J., Corrêa, I.C.S., Fontoura, B.S.d., Mendes, P.R., Nóbrega, A.V. and Serpa, C.G. (2026) Rio Grande Relay Zone, Rio Grande do Sul Coastal Plain, Brazil: I—Retiro-Estreito Main Fault and Sedimentation on Subsidence. *Open Journal of Geology*, **16**, 308-331. https://doi.org/10.4236/ojg.2026.167017

[10] Santos, A.C.O. (2020) Tectônica Gravitacional no Cone do Rio Grande, Bacia de Pelotas (RS). Ph.D. Thesis, Universidade Federal do Rio Grande.

[11] Tomazelli, L.J. and Villwock, J.A. (1996) Quaternary Geological Evolution of Rio Grande do Sul Coastal Plain, Southern Brazil. *Anais da Academia Brasileira Ciências*, **68**, 373-382.

[12] Tomazelli, L.J., Dillenburg, S.R. and Villwock, J.A. (2000) Late Quaternary Geological History of Rio Grange do Sul Coastal Plain, Southern Brazil. *Revista Brasileira de Geociências*, **30**, 474-476. https://doi.org/10.25249/0375-7536.2000303474476

[13] Rosa, M.L.C.D.C., Barboza, E.G., Abreu, V.D.S., Tomazelli, L.J. and Dillenburg, S.R. (2017) High-Frequency Sequences in the Quaternary of Pelotas Basin (Coastal Plain): A Record of Degradational Stacking as a Function of Longer-Term Base-Level Fall. *Brazilian Journal of Geology*, **47**, 183-207. https://doi.org/10.1590/2317-4889201720160138

[14] Milana, J.P., Guedes, C.C.F. and Buso, V.V. (2017) The Coastal Ridge Sequence at Rio Grande do Sul: A New Geoarchive for Past Climate Events of the Atlantic Coast of Southern Brazil since the Mid Holocene. *Quaternary International*, **438**, 187-199. https://doi.org/10.1016/j.quaint.2016.11.029

[15] Godolphim, M.F. (1985) Paleografia da Região do Cassino no Município de Rio Grande, BR. *Pesquisas em Geociências*, **17**, 233-254. https://doi.org/10.22456/1807-9806.21700

[16] Long, T. and Paim, P.S.G. (1987) Modelo de evolução histórica e holocênica do estuário da Lagoa dos Patos. 1˚ *Congresso da Associação Brasileira de Estudos do Quaternário*, Porto Alegre, 6-12 July 1987, 227-248.

[17] Corrêa, I.C.S., Aliotta, S. and Weschenfelder, J. (2004) Estrutura e Evolução dos Cordões Arenosos Pleistocênicos no Canal de Acesso à Laguna dos Patos-RS, Brasil. *Pesquisas em Geociências*, **31**, 69-78. https://doi.org/10.22456/1807-9806.19574

[18] Dillenburg, S.R., Barboza, E.G., Rosa, M.L.C.C., Caron, F. and Sawakuchi, A.O. (2017) The Complex Prograded Cassino Barrier in Southern Brazil: Geological and Morphological Evolution and Records of Climatic, Oceanographic and Sea-Level Changes in the Last 7-6 Ka. *Marine Geology*, **390**, 106-119.

https://doi.org/10.1016/j.margeo.2017.06.007

[19] Miranda, L.O.S. (1970) Geologia das bacias na Plataforma Sul-Brasileira. 1970 24*th Congresso Brasileiro de Geologia*, Brasília (Brazil), 20-26 September 1970, 129-140.

[20] Kowsmann, R., Leyden, R. and Francisconi, O. (1977) Marine Seismic Investigations, Southern Brazil Margin. *AAPG Bulletin*, **61**, 546-557. https://doi.org/10.1306/c1ea3d84-16c9-11d7-8645000102c1865d

[21] Rosendahl, B.R. (1987) Architecture of Continental Rifts with Special Reference to East Africa. *Annual Review of Earth and Planetary Sciences*, **15**, 445-503. https://doi.org/10.1146/annurev.ea.15.050187.002305

[22] Rosendahl, B.R., Kilembe, E. and Kaczmarick, K. (1992) Comparison of the Tanganyika, Malawi, Rukwa and Turkana Rift Zones from Analyses of Seismic Reflection Data. *Tectonophysics*, **213**, 235-256. https://doi.org/10.1016/0040-1951(92)90261-4

[23] Strieder, A.J., Heemann, R., Reginato, P.A.R., Acauan, R.B., de Amorim, V.A. and Remde, M.Z. (2015) Jurassic-Cretaceous Deformational Phases in the Paraná Intracratonic Basin, Southern Brazil. *Solid Earth Discussions*, **7**, 1263-1314. https://doi.org/10.5194/sed-7-1263-2015

[24] Ingersoll, R.V. (2012) Tectonics of Sedimentary Basins, with Revised Nomenclature. In: Busby, C. and Azor, A., Eds., *Tectonics of Sedimentary Basins*: *Recent Advances*, Blackwell Publishing Ltd., 1-43. https://doi.org/10.1002/9781444347166.ch1

[25] Varnes, D.J. (1978) Slope Movements Types and Processes. In: Schuster, R.L. and Krizek, R.J., Eds., *Landslides*: *Analysis and Control. Special Report* 176, Transportation Research Board, 11-35.

[26] Alves, T.M. (2015) Submarine Slide Blocks and Associated Soft-Sediment Deformation in Deep-Water Basins: A Review. *Marine and Petroleum Geology*, **67**, 262-285. https://doi.org/10.1016/j.marpetgeo.2015.05.010

[27] Sitter, L.U.D. (1954) Gravitational Gliding Tectonics, an Essay on Comparative Structural Geology. *American Journal of Science*, **252**, 321-344. https://doi.org/10.2475/ajs.252.6.321

[28] Bott, M.H.P. (2013) Mechanisms of Subsidence at Passive Continental Margins. In: Bally, A.W., Bender, P.L., McGetchin, T.R. and Walcott, R.I., Eds., *Dynamics of Plate Interiors*, American Geophysical Union, 27-35. https://doi.org/10.1029/gd001p0027

[29] Peel, F.J. (2014) The Engines of Gravity-Driven Movement on Passive Margins: Quantifying the Relative Contribution of Spreading vs. Gravity Sliding Mechanisms. *Tectonophysics*, **633**, 126-142. https://doi.org/10.1016/j.tecto.2014.06.023

[30] Zwaan, F., Rosenau, M. and Maestrelli, D. (2021) How Initial Basin Geometry Influences Gravity-Driven Salt Tectonics: Insights from Laboratory Experiments. *Marine and Petroleum Geology*, **133**, Article ID: 105195. https://doi.org/10.1016/j.marpetgeo.2021.105195

[31] Zhang, J., Wu, S., Hu, G., Yue, D., Xu, Z., Chen, C., *et al.* (2021) Role of Shale Deformation in the Structural Development of a Deepwater Gravitational System in the Niger Delta. *Tectonics*, **40**, e2020TC006491. https://doi.org/10.1029/2020tc006491

[32] dos Reis, A.T., Silva, C.G., Gorini, M.A., Leão, R., Pinto, N., Perovano, R., *et al.* (2016) The Chuí Megaslide Complex: Regional-Scale Submarine Landslides on the Southern Brazilian Margin. In: Lamarche, G., *et al.*, Eds., *Submarine Mass Movements and Their Consequences*, Springer, 115-123. https://doi.org/10.1007/978-3-319-20979-1_11

[33] Assumpção, M., Dourado, J.C., Ribotta, L.C., Mohriak, W.U., Dias, F.L. and Barbosa, J.R. (2011) The São Vicente Earthquake of 2008 April and Seismicity in the Continental Shelf off SE Brazil: Further Evidence for Flexural Stresses. *Geophysical Journal Inter-*

*national*, **187**, 1076-1088. https://doi.org/10.1111/j.1365-246x.2011.05198.x

[34] Contreras, J. (2011) Seismo-Stratigraphy and Numerical Basin Modeling of the Southern Brazilian Continental Margin (Campos, Santos, and Pelotas Basins). Tese de Doutor da Faculdade de Ciências Naturais e Matemáticas, Ruprecht-Karls-University.

[35] Prior, D.B. and Coleman, J.M. (1978) Disintegrating Retrogressive Landslides on Very-Low-Angle Subaqueous Slopes, Mississippi Delta. *Marine Geotechnology*, **3**, 37-60. https://doi.org/10.1080/10641197809379793

[36] Kunz, B.F.J. (1960) Diffraction Problems in Fault Interpretation. *Geophysical Prospecting*, **8**, 381-388. https://doi.org/10.1111/j.1365-2478.1960.tb01722.x

[37] Krey, T. (1961) The Significance of Diffraction in the Investigation of Faults. *Geophysical Prospecting*, **9**, 77-92. https://doi.org/10.1111/j.1365-2478.1961.tb01691.x

[38] Reynolds, J.M. (2011) An Introduction to Applied and Environmental Geophysics. 2nd Edition, John Wiley & Sons, 596 p.

[39] Vespremeanu-Stroe, A., Preoteasa, L., Zăinescu, F., Rotaru, S., Croitoru, L. and Timar-Gabor, A. (2016) Formation of Danube Delta Beach Ridge Plains and Signatures in Morphology. *Quaternary International*, **415**, 268-285. https://doi.org/10.1016/j.quaint.2015.12.060

[40] Jol, H.M. and Smith, D.G. (1991) Ground Penetrating Radar of Northern Lacustrine Deltas. *Canadian Journal of Earth Sciences*, **28**, 1939-1947. https://doi.org/10.1139/e91-175

[41] Sjögren, P. (2009) Sand Mass Accumulation Rate as a Proxy for Wind Regimes in the SW Barents Sea during the Past 3 Ka. *The Holocene*, **19**, 591-598. https://doi.org/10.1177/0959683609104033

[42] Yang, N., Zhang, J., Cai, Y., Feng, Y., Yang, L., Cheng, H., *et al.* (2022) Timing and Implications of Aeolian Sand Accumulation in a Alpine Basin of Qilian Shan, NE Qinghai-Xizang Plateau. *Frontiers in Earth Science*, **10**, Article 939887. https://doi.org/10.3389/feart.2022.939887

[43] Rymer, K.G., Rachlewicz, G., Buchwal, A., Temme, A.J.A.M., Reimann, T. and van der Meij, W.M. (2022) Contemporary and Past Aeolian Deposition Rates in Periglacial Conditions (Ebba Valley, Central Spitsbergen). *Catena*, **211**, Article ID: 105974. https://doi.org/10.1016/j.catena.2021.105974

[44] Oliver, T.S.N. (2016) Holocene Depositional History of Three Coastal Sand Ridge Plains, Southeastern Australia. Ph.D. Thesis, University of Wollongong, 216 p. https://ro.uow.edu.au/cgi/viewcontent.cgi?article=5657&context=theses

[45] Holliday, S.E., Klein, C.J., Nichols, M. and Brouwer-Riel, C. (1993) Surficial Sediments in Mid-Atlantic Estuaries. NOAA, National Ocean Service, National Estuarine Inventory, 70 p. https://repository.library.noaa.gov/view/noaa/47491/noaa_47491_DS1.pdf

[46] Adojoh, O., Marret-Davis, F., Osterloff, P., Hart, M., Ikuenobe, F., Weakley, H., *et al.* (2024) Sedimentation Rates, Coastal Delta Accretion, and Stratigraphic Datum of the Late Pleistocene-Mid-Holocene Transition in the East Equatorial Atlantic: New Concept from Calcareous Nannoplankton. *The Holocene*, **35**, 409-419. https://doi.org/10.1177/09596836241307303

[47] Restreppo, G.A., Wood, W.T. and Phrampus, B.J. (2020) Oceanic Sediment Accumulation Rates Predicted via Machine Learning Algorithm: Towards Sediment Characterization on a Global Scale. *Geo-Marine Letters*, **40**, 755-763. https://doi.org/10.1007/s00367-020-00669-1

[48] Peacock, D.C.P., Knipe, R.J. and Sanderson, D.J. (2000) Glossary of Normal Faults.

*Journal of Structural Geology*, **22**, 291-305.
https://doi.org/10.1016/s0191-8141(00)80102-9

[49] Peacock, D.C.P., Nixon, C.W., Rotevatn, A., Sanderson, D.J. and Zuluaga, L.F. (2017) Interacting Faults. *Journal of Structural Geology*, **97**, 1-22.
https://doi.org/10.1016/j.jsg.2017.02.008

[50] Poulimenos, G., Zelilidis, A., Kontopoulos, N. and Doutsos, T. (1993) Geometry of Trapezoidal Fan Deltas and Their Relationship to Extensional Faulting along the South-western Active Margins of the Corinth Rift, Greece. *Basin Research*, **5**, 179-192.
https://doi.org/10.1111/j.1365-2117.1993.tb00064.x

[51] Pichel, L.M., Antunes, A.F., Fossen, H., Rapozo, B.F., Finch, E. and Córdoba, V.C. (2022) The Interplay between Basement Fabric, Rifting, Syn-Rift Folding, and Inversion in the Rio Do Peixe Basin, NE Brazil. *Basin Research*, **35**, 61-85.
https://doi.org/10.1111/bre.12704

[52] Roche, V., Camanni, G., Childs, C., Manzocchi, T., Walsh, J., Conneally, J., *et al.* (2021) Variability in the Three-Dimensional Geometry of Segmented Normal Fault Surfaces. *Earth-Science Reviews*, **216**, Article ID: 103523.
https://doi.org/10.1016/j.earscirev.2021.103523

[53] Williams, G. and Vann, I. (1987) The Geometry of Listric Normal Faults and Deformation in Their Hangingwalls. *Journal of Structural Geology*, **9**, 789-795.
https://doi.org/10.1016/0191-8141(87)90080-0

[54] Peacock, D.C.P. and Sanderson, D.J. (1994) Geometry and Development of Relay Ramps in Normal Fault Systems. *AAPG Bulletin*, **78**, 147-165.
https://doi.org/10.1306/bdff9046-1718-11d7-8645000102c1865d

[55] Pickering, G., Peacock, D.C.P. and Lee, J.M. (1997) Modeling Tip Zones to Predict the Throw and Length Characteristics of Faults. *AAPG Bulletin*, **81**, 82-99.
https://doi.org/10.1306/522b4299-1727-11d7-8645000102c1865d

[56] White, I.R. and Crider, J.G. (2006) Extensional Fault-Propagation Folds: Mechanical Models and Observations from the Modoc Plateau, Northeastern California. *Journal of Structural Geology*, **28**, 1352-1370. https://doi.org/10.1016/j.jsg.2006.03.028

[57] Childs, C., Holdsworth, R.E., Jackson, C.A.L., Manzocchi, T., Walsh, J.J. and Yielding, G. (2017) Introduction to the Geometry and Growth of Normal Faults. *Geological Society, London, Special Publications*, **439**, 1-9. https://doi.org/10.1144/sp439.24

[58] Hance, J.J. (2003) Development of a Database and Assessment of Seafloor Slope Stability Based on Published Literature. Master's Thesis, University of Texas at Austin (USA), 245 p.

[59] Shanmugam, G. (2018) Slides, Slumps, Debris Flows, Turbidity Currents, and Bottom Currents: Implications. In: Shanmugam, G., Ed., *Reference Module in Earth Systems and Environmental Sciences*, Elsevier, 49 p.
https://doi.org/10.1016/b978-0-12-409548-9.04380-3